UNIVERSITY OF CALIFORNIA
RIVERSIDE

Nonlinear Transmission Impairments in High-Spectral Efficiency Fiber-Optic Communications

A Dissertation submitted in partial satisfaction
of the requirements for the degree of

Doctor of Philosophy

in

Electrical Engineering

by

Yi-Hsiang Wang

August 2011

Dissertation Committee:
Dr. Ilya Dumer, Chairperson
Dr. Ilya Lyubomirsky
Dr. Roger Lake

The Dissertation of Yi-Hsiang Wang is approved:

_____

_____

_____

Committee Chairperson

University of California, Riverside

Acknowledgments

From the initial decision to the final completion, this dissertation would not have been possible without the guidance and support of several individuals.

First and foremost, I am heartily thankful to my supervisor, Dr. Ilya Lyubomirsky, who gave me time and resources to explore this field, as well as his wise advice and continuous encouragement during these years.

I would also like to thank Dr. Ilya Dumer and Dr. Roger Lake for their time and efforts on serving as my committee, especially for Dr. Ilya Dumer's generous assistance to complete the final process of my PhD.

I would also like to thank Eric Chien and Eric Chang for giving me so many great suggestions for my proposal and presentations, as well as sharing their valuable experiences on lab experiments and on life. Gregory Liu, Kyle Pi, Hank Huang, Wu-Feng Yah, Roy Kwon, Morgan Zhang, Kevin Zhang, Chris Tsai, Pearl Chen, Valerie Chen, and many other friends, who generously gave their friendships and really enriched my life at Riverside. The past five years would not be fun without these folks.

Lastly, I truly thank my grand aunt, Lichu, for her great care, my parents for their unconditional support, and my lovely family for their love.

ABSTRACT OF THE DISSERTATION

Nonlinear Transmission Impairments in High-Spectral Efficiency
Fiber-Optic Communications

by

Yi-Hsiang Wang

Doctor of Philosophy, Graduate Program in Electrical Engineering
University of California, Riverside, August 2011
Dr. Ilya Dumer, Chairperson

This dissertation is designed to focus on the field of nonlinear impairments generated along the fiber-optic transmission links in high spectral efficiency optical modulation systems, while also extracting the performance trade-offs of conventional and novel receivers. Fundamental knowledge of optical fiber, major phase modulation nonlinearities, and high spectral efficiency optical modulation and reception are discussed on an introductory level. Further, balanced detection schemes for optical duobinary with a comparison of differential phase shift keying (DPSK) are demonstrated and analyzed, both in simulations and experiments. Frequency discriminator receiver structures for quadrature phase shift keying (QPSK) as well as their linear and nonlinear noise properties are exhibited. At the end, polarization multiplexing QPSK with digital coherent receiver well known as future vision of fiber-optic communications is also simulatedly studied through the RZ- and NRZ- pulse shape impact in a 9–channel 100G wavelength division multiplexing (WDM) systems.

Table of Contents

Lists of Figures

Chapter 1
Introduction

The improvements of global telecommunications have been quietly changed today's society, expanding World Wide Web to every corner of the world. Variety of online services, creative business ideas, and information resources can be found inside this virtual universe. This change reduces the cost of long distance communications easier, alongside forming new business models. Later on, popularizations of telecommunication such as optical fiber to home (OFTH), Wi-Fi, and 3G/4G network enable internet to be received much faster and wider. In this alternative age, even though many people do not realize it, optical transmission has played a tremendous role.

1.1 Global Telecommunication

Figure 1.1 describes a simple structure of global telecommunication network. It contains access network, metropolitan (or regional) network, and long haul core network. Depending on the hierarchy of network, it is employed in different communications [1]. Long-haul core network, also known as backbone network, is set up for long distance networking such as transnational connection, transoceanic transmission, and global coverage. It usually spans the longest distance (> 1000 km), connecting multiple metro networks. Expanding data capacity within limited bandwidth and extending transmission distance with less energy regeneration are always the main concerns of core network. Apparently, fiber-optic communication is still the most suitable for such a long-haul

transmission link right now. Low power loss (~0.2 dB/km) can reduce the cost of amplifier, while high system capacity of optical wavelength division multiplexing (WDM) systems can pack highly condensed information in a single wire. Thus, optical fiber supports most backbone network today.

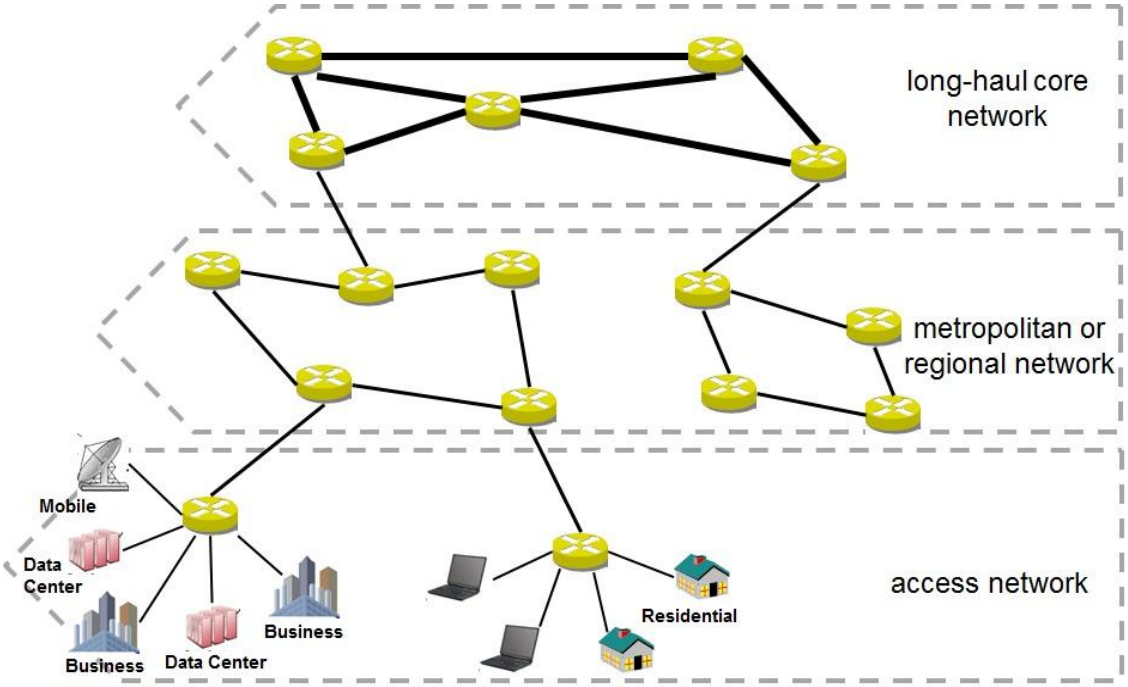

Figure 1.1 Global Telecommunications

Metro-area network provides data transport within a shorter distance (< 300 km) or across a smaller area (300 ~ 1000 km). A metropolitan network is the bridge built for communicating the long-haul core network and connecting numbers of access networks. Although the traffic of data transport is much smaller than long-haul core network, a large amount of exchange points results in another challenge that the switching architecture is concerned as a larger cost in a such complex network.

Moving down to the bottom of the whole hierarchy in Figure 1.1, it is the access network that supports end-users spreading around the whole world. Various technologies for end-user applications are available through different transmitting medium such as copper wire of digital subscriber line (DSL), wireless of Wi-Fi, and optical fiber of fiber-to-home service. Due to the advantage of wider bandwidth over cooper wire, optical fiber enables high speed data transmission as well as lower loss that guarantees the quality of transmitted signals.

1.2 Motivations

Long-haul fiber optic transmission system may seem like a mature technology, being employed in the core or metro network of global telecommunications. However, the pursuit of high spectral efficiency has not been diminished due to the ever-increasing global internet traffic. A new IEEE standard was soon announced in 2006 for 40G synchronous optical network (SPNET)/ 100G Ethernet. That means the next generation of transmission links will be 40 Gb/s or 100 Gb/s per wavelength channel, which causes efficiency between 0.8 and 2.0 b/s/Hz [2]. Such a high spectral efficiency condenses channel spacing, displays different tastes for modulation formats, as well as inducing stronger nonlinear impairments.

In this thesis, we first focus on the balanced detection schemes for optical duobinary that exhibits more compact spectrum to achieve Nyquist limit, compared to DPSK. In addition, 40-Gb/s polarization multiplexing DQPSK (Polmux-DQPSK) is discussed.

Finally, 9-channel WDM 100G Polmux QPSK will be studied. These three topics will be discussed in both linear and nonlinear regimes.

1.2.1 Milestone of Fiber-Optic Communications

Due to the globalization of internet, World Wide Web (WWW) is not just a luxury but a necessity. At the same time, a new economy and evolved business model distribution are changing life styles of human beings. This increased demand to the internet bandwidth is accelerating the evolution of Fiber-Optic communications. In late November 2006, a new technical challenge of Ethernet speed after 10 Gigabit has been approved by the IEEE Higher Speed Study Group (HSSG) [3]. The next generation of Ethernet speed jumped from 10 Gigabit to 100 Gigabit. This quick rising tide of bandwidth needs is driven by the high-intense bandwidth applications such as high performance computing, high definition videos on demand, virtualization, IP traffic, and network attached storage. However, like 40G SONET, several vendors initialed a push to include a 40 Gigabit in the standard in 2007. IEEE 802.3ba, the first standard including two different Ethernet speeds, was named in the late 2007 [4].

In addition, the spectral efficiency is a key consideration in 40G or 100G optical transmission systems. Theoretically, it is achievable for binary modulation to reach 1 b/s/Hz, but spectral efficiency is still lower in practice because the noise source induced by self-phase modulation and crosstalk from neighboring channels. Modulation formats, such as duobinary and DPSK, display a better tolerance to narrow optical filtering and enable 0.8-b/s/Hz spectral efficiency [2]. Polmux DQPSK displays a good performance

in 40 Gb/s competition. In 100G WDM system, Polmux-QPSK seems to be a suitable selection in combination of digital signal processing and coherent detection. To figure out the next generation of fiber-optic communication, nonlinear impairment can't be neglected.

1.2.2 Internet Traffic

The rapid growth of internet traffic has challenged the techniques of global telecommunications, and optic-fiber communication is no exception. The larger demand on internet facilities, the higher spectral efficiency is chased. According to Cisco global IP traffic forecast and methodology in Figure 1.2, internet traffic will exceed 767 exabytes (1 EB=1 billion gigabytes) in four years [5, 6]. In 2009, global internet traffic grew 45% and reached 176 EB which mobile network did not occupy more than 1%. As 3G/4G mobile network has become more popular, it is estimated to expand to 4% in 2014. Large amount of file sharing, variable videos uploaded and downloaded on different online planes such as YouTube [7], and the increasing web data because of the new type of social network like Facebook [8] are also the factors of the internet traffic. In the future, as the hardware improves, cloud computing may turn into a success and become a heavy weight factor of IP traffic. In order to support such a demand to internet bandwidth, expanding the capacity of information in the optical transmission is not only necessary but is urgently needed.

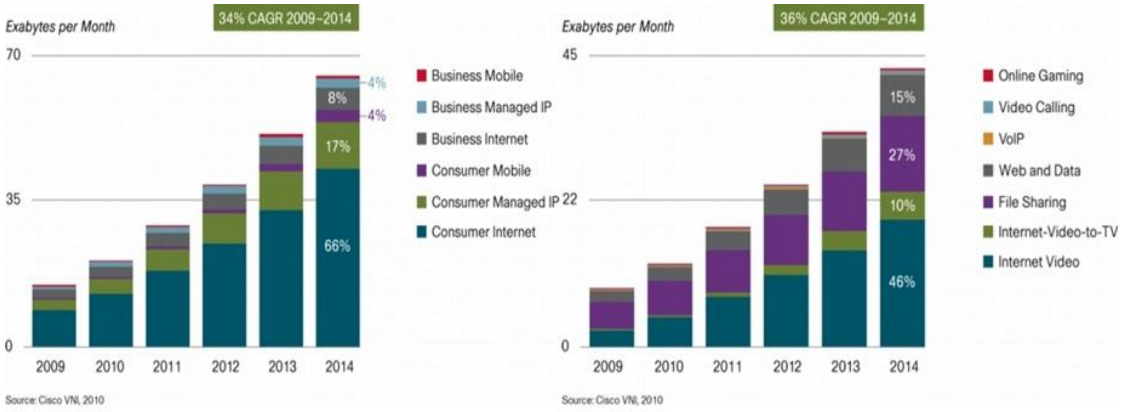

Figure 1.2 IP traffic forecast

1.3 Objectives

The research discussed in this thesis studies three major nonlinear effects that might strongly influence 40G/100G optical transmission system that ideally will be competitive to 10-Gb/s system. First topic, the impact of nonlinear phase noise induced by the combination of optical Kerr effect and self-phase modulation (SPM) accumulates in single channel with high system capacity. Secondly, cross phase modulation (XPM), which can be described as crosstalk with neighboring channels, will be illustrated. Finally, nonlinear polarization scattering or polarization scattering (XPOLM) will be discussed.

In particular, this dissertation also discusses balanced detection schemes for optical duobinary which can be seen as a strongly filtered DPSK. The narrower spectrum bandwidth and better tolerance to optical filtering might admit optical duobinary to pace in next generation fiber-optic communication systems.

The entire work described in this thesis has been carried out at Photonic Systems and Devices Laboratory in department of Electrical Engineering of University of California, Riverside.

1.4 Outline of this thesis

The first part of this thesis includes Chapter 2, 3 and 4, which focus on long-haul WDM transmission system, major nonlinear effects, and modulation formats.

The second part consists of Chapter 5 to 7, which discuss the experimental and simulated results of linear and nonlinear effects in optical duobinary, Polmux-DQPSK, and Polmux-QPSK systems.

Chapter 2
Long-haul WDM Fiber-Optic Transmission Systems

Wavelength Division Multiplexing (WDM) is the most popular channel multiplexing technique because this technique enables multiplication of system capacity without laying more optical fibers in optical communication systems. It is also attractive that several generations of transmission technology can coexist in a WDM system without having overhauls of optical networks. By using this technique, optical carriers at different wavelengths are multiplexed onto a single optical fiber or an optical medium, overcoming the limitations imposed by dispersion, nonlinear effects, and electronic component speeds in a single channel [9-11]. For instance, a total 25.6 Tb/s transmission over a single mode fiber can be achieved by using 160 WDM channels of 85.4-Gb/s polarization multiplexed RZ-DQPSK on 50 GHz channel spacing [12]. Thus, under an expected desire to system capacity and cost reduction in the future, modern researches should be developed toward the deployment in long-haul WDM transmission systems.

This chapter is organized as follows. In section 2.1, we focus on a long-haul WDM fiber-optic transmission scheme in which basic fiber structures, attenuation, and optical amplifiers are implemented. Sections 2.2-2.3 discuss the linear impairments, amplifier spontaneous emission noise, and chromatic dispersion, respectively. Section 2.4 explains the ideas of dispersion compensation.

2.1 Long-Haul WDM Transmission System Scheme

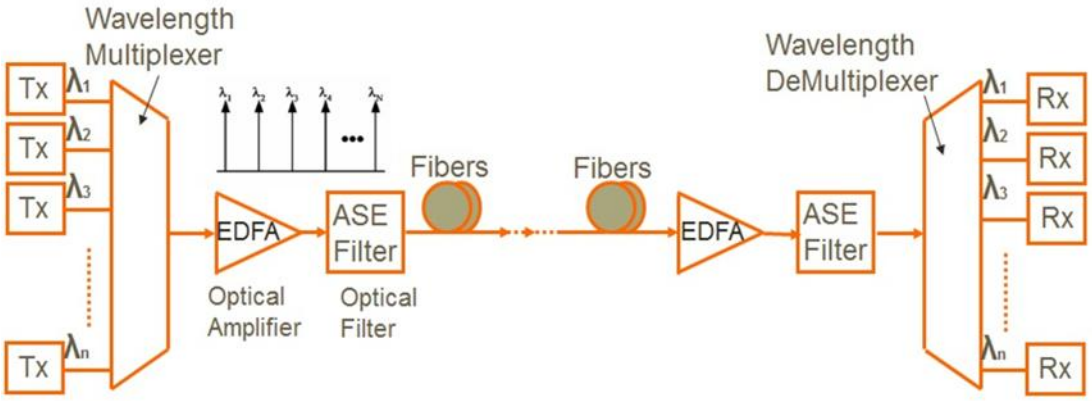

Figure 2.1 Long-haul WDM transmission system

Error! Reference source not found. schematically describes the fundamental structure f WDM lightwave system. Each transmitter converts the information data onto optical carriers generated by lasers, determining the modulation formats and transmission bitrate. The modulated optical carriers operating at different wavelengths are combined by a wavelength multiplexer such as an arrayed waveguide grating (AWG) in which the channel-interleaved space is a key parameter of system design for system capacity and tolerance to the impairments. Experimentally, the channel interleaving of 50 GHz channel spacing can allow up to 200 channels in long-haul transmission, and 80-channel density of WDM channels is currently the most advanced technique. Smaller channel spacing allows the system to pack more transmitted information but might increase the strength of linear or nonlinear effects, which would be explained in the next chapter.

In such a WDM system, the modulation formats decides the most characteristics of optical signals such as OSNR sensitivity, tolerance chromatic dispersion, and the

influence of fiber nonlinearities. Today, the transmission bitrate is jumping from 10 Gb/s to next generation of 40 Gb/s per channel, expectedly heading forward to the next generation of 100 Gb/s per channel as well [13-15]. In such a high spectral efficiency transmission system such as 40-Gb/s DPSK or DQPSK and 100-Gb/s Polmux-QPSK, the impact of nonlinear impairments is turning into a key role of system design.

The optical transmission paths are usually built by several elements, fibers, ASE filters, and optical amplifiers in cascade. Power budget is the first consideration to maintain the performance of each receiver while the loss limitation eventually reduces transmission distance. The use of optical amplifier is one of the approaches to overcome the limitation. During 1980s, several kinds of optical amplifiers have been discovered, but Erbium-Doped Fiber Amplifier (EDFA) operating at ~1550 nm draws the most attentions among regenerators. Some transmission impairments such as amplifier spontaneous emission (ASE) noise and chromatic dispersion (CD) also have to be compensated by the modifications of link design. Thus, an optical amplifier followed by an optical noise filter and single mode fibers combined with DCF before or after are inserted into transmission links. At the receiver end, the wavelength demultiplexer separates the output signal back to each optical carrier at its corresponding wavelength for demodulation.

2.1.1 Fibers

The structure of an optical fiber can be simply described as a cylindrical core of silica glass surrounded by a cladding with the refractive index which is lower than the refractive index. Optical fibers act like circular dielectric waveguides guiding light

through total internal reflections. This application of using silica glass as a practical medium for communications was first proposed by Kao and Hockham in 1966 [16]. After years passed, either manufacturing or material technology has been improved for enabling fiber optic communications to expand and progress.

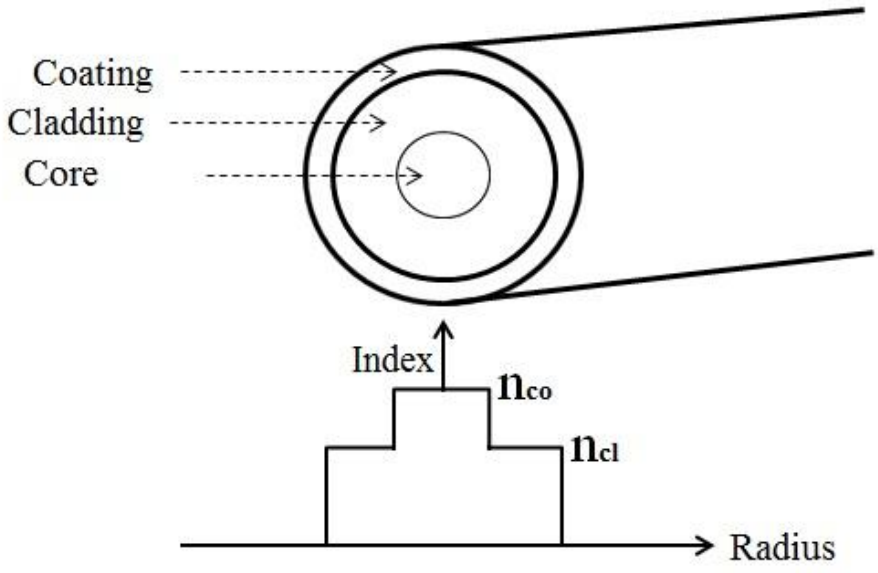

Figure 2.2 Cross section of silica fibers

Figure 2.2 shows the cross section of a silica fiber. The core surrounded by the cladding is at the center of an optical fiber where optical carriers are bounded and transmitted. The coating is necessary for protection of the fibers. With a larger difference between two refractive indices, the core-cladding interface is able to confine maximum light into the fibers, which allows multiple modes of lights transfer over the core. This type of fiber is called multimode fiber. However, multipath dispersion is so induced and leads to considerable pulse broadening along the fibers, which contributes to different paths for

different rays. This impairment doesn't appear in single mode fibers, which is also the key advantage of single mode fibers. We only consider single mode fiber in this paper.

Single mode fibers made also by silica guide only one transvers mode with two orthogonal polarizations. The refractive index of the core is ~1.48, which is ~0.5% higher than the refractive index of the cladding. This low refractive index difference enables optical signals well confined in the core, while reducing the loss induced by scattering as well. The typical diameter of the fiber core is ~8 μm with cut-off frequency ~1260 nm.

In the coming sections, we also discussed the physical properties of single mode fibers most related to long-haul transmission systems.

2.1.2 Attenuation

Optical power loss caused by the scattering and absorption in the optical fiber is the most fundamental limitation to the long-haul optical communication systems. Noting that the fiber loss varies with the wavelength of light, the attenuation as a function of wavelength is shown in Figure 2.3. Material absorption combined with scattering generates a bending curve with the lowest loss around 1550 nm wavelength range. For long-haul transmission, ~0.2 dB/km fiber loss allows power regeneration every ~ 100km span.

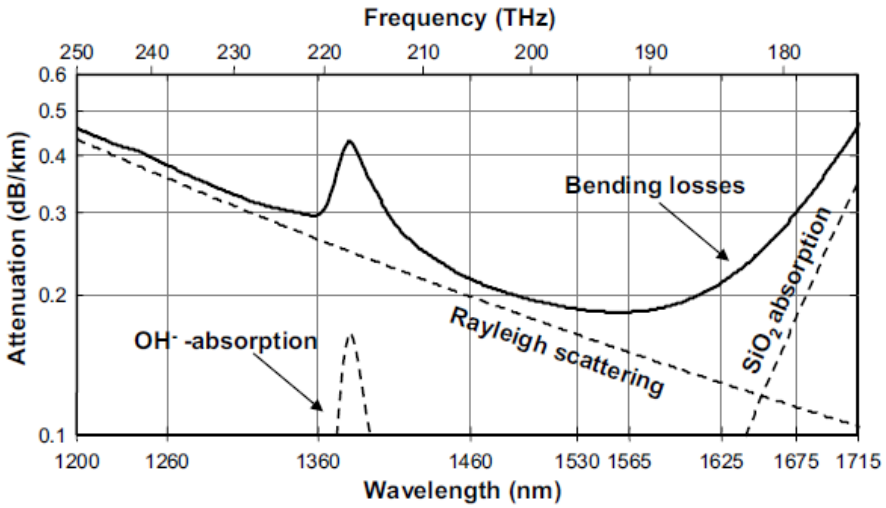

Figure 2.3 Attenuation of silica fibers

If P_0 is the input optical power of a fiber of length L, the transmitted power P_L can be given by

$$P_L = P_0 e^{-\alpha L}$$

where α is the attenuation constant measured through total fiber loss. It is able to be customary in units of dB/km using

$$\alpha_{dB} = -\frac{10}{L}\log\left(\frac{P_L}{P_0}\right) = 4.343\alpha$$

where α_{dB} is α in dB/km. In this thesis, is the attenuation constant in units of dB/km will be used unless noticed.

2.1.3 Mach-Zehnder Modulation (MZM)

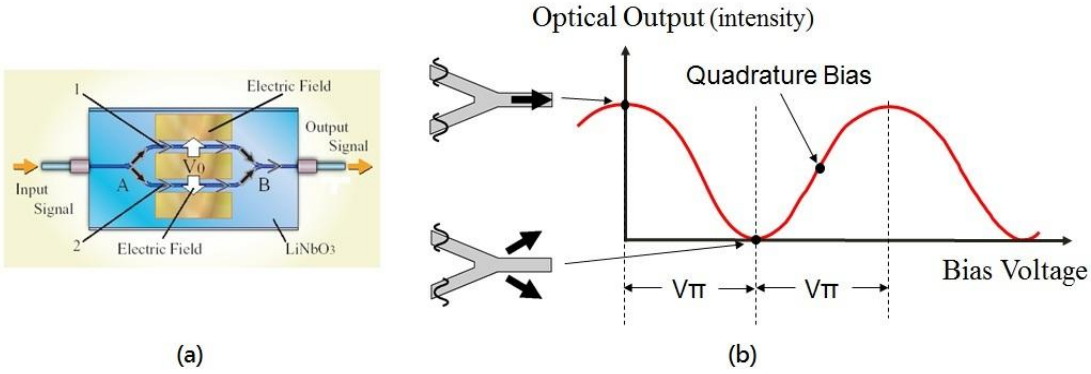

Figure 2.4 Mach-Zehnder modulator (MZM)

Mach-Zehnder modulator (MZM) is the most widely used device for optical modulation. As shown in Figure 2.4 (a), a MZM consists of two equal length waveguides and a coupler at the output end to create am interferometer. The incident light passes through two equal paths, which are normally made by Lithium-Niobate (LiNbO**3**) electro-optic crystal. In such an electro-optic crystal, the refractive index is in response to the applied electric field. On the other hand, by controlling the electrical drive voltages, it is able to modulate the refractive index of incident lights, converting the signals from electrical domain to optical domain.

A typical transmission curve of interference generated by the coupler in a MZM is demonstrated in Figure 2.4 (b). The additional phase shift induced by the difference of the electrical drive voltages added on the two waveguides can change the interference to either constructive or destructive. If the phase difference is equal to π, there is no light transmitted out of the modulator due to the destructive interference. Without the phase

shift, the modulator experiences interference constructively. In general, the difference of drive voltage to switch interference between constructive and constructive is known as V_π. If the input signal splits into two equal electric fields $\frac{1}{\sqrt{2}}E_i$ via Y junction, the combined signal at the output end can be described as

$$E_o = \frac{Ei}{2}\left[\exp\left(j\pi\frac{V_1(t)}{2V_\pi}\right) - \exp\left(j\pi\frac{V_2(t)}{2V_\pi}\right)\right]$$

In high speed optical transmission system, MZM is particularly suitable for conversation between optical and electrical signals at transmitter as low insertion loss (~4 dB) that is barely influenced by wavelength, the high electro-optic bandwidth, and high extinction ratio.

2.2 EDFA & ASE Noise

Erbium doped fiber amplifier (EDFA) is a widely used optical amplifier with a broad regeneration bandwidth at the wavelength region around 1550 nm area at which standard single mode fibers operate. The use of fiber-doped amplifier became practical since 1990, after the manufacturing techniques were improved. Recently, the development of optical amplification technology based on erbium doped fiber amplifier (EDFA) allows for 100-1000 optical channels to be amplified simultaneously without electrical regeneration [17-19]. This deployment of EDFA in WDM system brought a revolution of the fiber-optic communication systems.

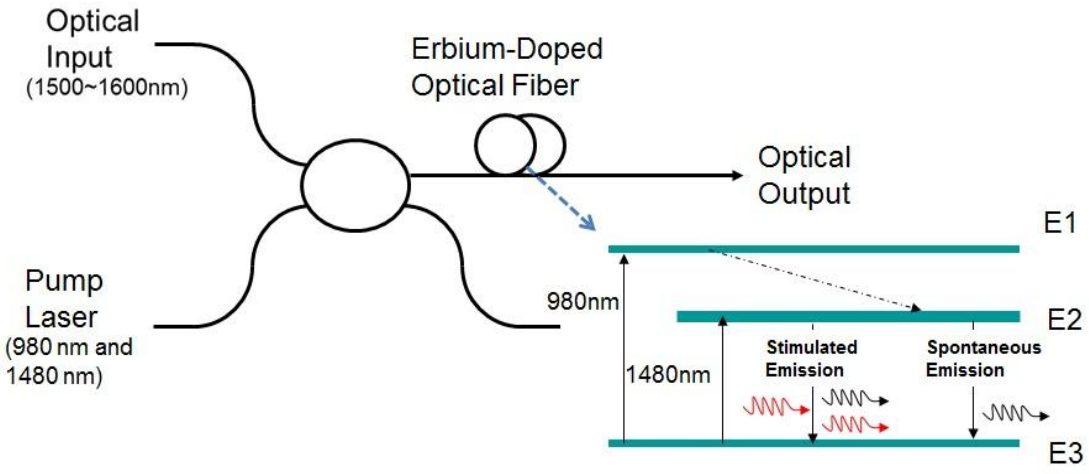

Figure 2.5 Structure of Erbium Doped Fiber Amplifier

In Figure 2.5, the process of optical power regeneration in EDFA is briefly illustrated. The input optical signal and pump beams operation at different frequencies are launched into the fibers doped with Erbium ions (E_r^{+3}). The energy is transferred from pump beams to signal beams through stimulated emission. Inside the Erbium-doped fibers, population inversion is created by input pump energy to produce higher energy level photons. Efficient EDFA pumping is usually using the semiconductor lasers with operation wavelength at 980 nm and 1480 nm.

The noise induced by spontaneous emission shown in Figure 2.5 is called amplifier spontaneous emission (ASE). While optical signals propagate through Erbium-Doped fiber, not only the optical power is boosted periodically, but the spontaneous emission is generated simultaneously due to population inversion. The extra unwanted photons accumulated along the transmission line result in power fluctuations, which turns into noise in the optical communication systems. The ASE added during amplification of

optical power can reduce optical signal-to-noise ratio (OSNR). A practical EDFA usually has a noise figure ~4dB.

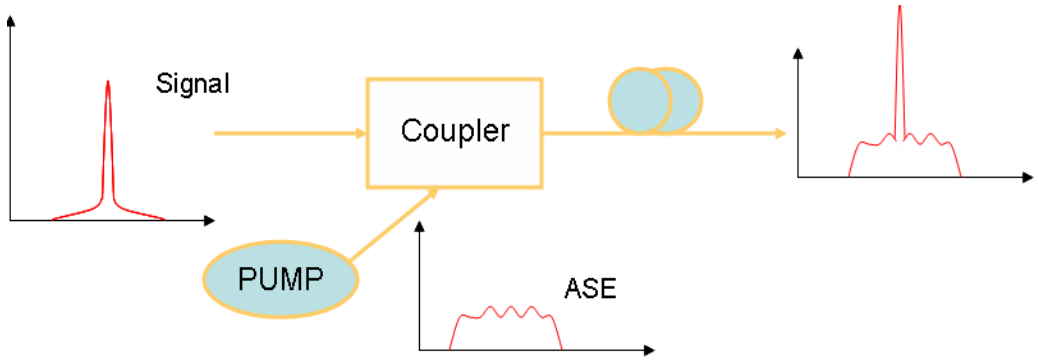

Figure 2.6 Amplifier Spontaneous Emission (ASE) Noise

This phenomenon can be simply explained in Figure 2.6. The optical carriers coupled with light of pump laser are launched into Erbium doped fiber. Population inversion caused by pump laser brings in both stimulated emission and spontaneous emission.

2.3 Chromatic Dispersion

Chromatic dispersion (CD) also called Group Velocity Dispersion (GVD) is another important impairment that relates to pulse broadening, resulting inter-symbol interference (ISI) during long-haul transmission. This limits the transmission distance without dispersion compensation mechanism, while restricting spectral efficiency especially for WDM systems. Here, we will discuss the basic concepts of chromatic dispersion and the influence on optical transmission systems. The impact on the design of transmission will be studied in next section.

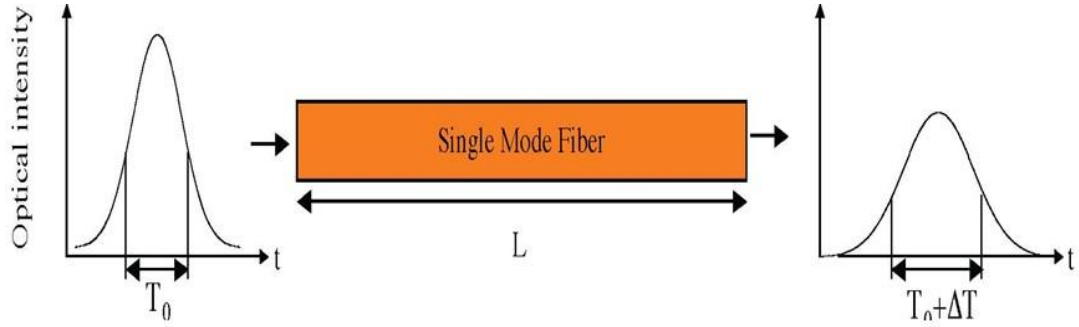

Figure 2.7 Chromatic Dispersion

In single mode fibers, multimode dispersion is absent, but pulse broadening does not disappear. It is notable that the transmitted signal pulse carrying 1s or 0s has a finite spectral bandwidth. The wavelength dependence of refractive index results in different travel velocities for different frequency components in an optical fiber. Thus, those signals of different frequency components propagate at different speeds and consequently do not arrive at the output end simultaneously.

A modulated optical signal contains the information and optical carriers. The optical carrier wave travel at guide phase velocity which can be described as

$$v_p = \frac{\omega}{\beta_z}$$

where ω is angular frequency and β_z is propagation constant. However, information propagate according to the group velocity

$$v_g = \left(\frac{\partial \beta_z}{\partial \omega}\right)^{-1}$$

For a plane wave traveling in glass of the refractive index n, $\beta = \mathrm{n}\frac{\omega}{c}$. Thus, group velocity can be written as

$$\frac{\partial \beta_z}{\partial \omega} = \frac{n}{c} + \frac{\omega}{c}\frac{\partial \mathrm{n}}{\partial \omega} = \frac{1}{c}\left(n + \omega\frac{\partial \mathrm{n}}{\partial \omega}\right) = \frac{n_g}{c}$$

where

$$v_g = \left(\frac{\partial \beta_z}{\partial \omega}\right)^{-1} = \frac{c}{n_g}$$

$$n_g = n + \omega\frac{\partial \mathrm{n}}{\partial \omega}$$

Group delay for single mode fiber

$$\Delta\tau = \frac{\partial \tau}{\partial \omega}\Delta\omega = \frac{\partial}{\partial \omega}\left(\frac{L}{v_g}\right)\Delta\omega = L\frac{\partial}{\partial \omega}\left(\frac{\partial \beta}{\partial \omega}\right)\Delta\omega = L\beta_2\Delta\omega$$

By changing the profile of refractive index, the chromatic dispersion and dispersion slope can be negative. This type of fibers is capable of dispersion compensation and referred to as dispersion compensation fiber (DCF). In next section, DCF and dispersion compensation map will be discussed.

2.4 Dispersion Compensation (DCF)

Chromatic dispersion accumulates along optical transmission links and causes ISI which restricts available transmission distance. In higher spectral efficiency, the limited reach can be smaller. This can be supported by Table 2.1 where the dispersion-induced

limitation varies is in response to baud rate. Therefore, to compensate chromatic is required.

Numbers of technologies were proposed and developed for dispersion compensation, such as dispersion compensation fibers (DCF), dispersion compensation module (DCM), Fiber Bragg gratings (FBG), and digital signal processing (DSP). In this section, we focus on DCF and DCM.

DCF first proposed by in 1980 [20], is today's standard application for compensating chromatic dispersion. As can be seen in Figure 2.x, DCF has a very small core effective area and different refractive index profile compared with SSMF. The refractive index profile of DCF has a three-level index cladding structure surrounding the high index and small area core. The small core size and 3-level index cladding constrain optical carriers to travel in the cladding, resulting in negative and large value of D. With the negative value of D, DCF is able to compensate chromatic dispersion generated by SSMF. However, small core area and optical fields propagating in cladding part can induce larger nonlinear coefficient and higher loss (α=~0.5 dB/km).

Besides DCF, dispersion compensation module (DCM) is another aspect of dispersion compensation. In DCM, the fiber is wound up a spool to produce discrete dispersion compensation, can provides a fixed value or a tunable amount of dispersion. The insertion loss of DCM, which is able to compensation the dispersion of 100 km SSMF (1700 ps/nm), is ~ 6dB. Thus, a two-stage EDFA is needed for using DCM to regenerate

energy. However, various properties of DCM such as distance-independent, tunable, or with lower intra channel nonlinear coefficient, still make DCM important.

Chapter 3
Nonlinear Impairments

In fiber-optic communications, noise or system performance degradations induced by nonlinear effects in optical fibers are known as nonlinear impairments. Since the observation of some nonlinear-optical phenomena such as Pockels and Kerr electro-optic effects [21], it has been well know that the interaction of intense light with any dielectric medium turns the response of the medium to the electromagnetic field into nonlinear. This type of nonlinear property happens without exceptions in optical fibers. Even though silica fiber is a weakly nonlinear medium, nonlinear impairments can turn into significant in fiber-optic communication system, especially for long-haul WDM fiber-optic transmission systems due to multiple channel mixing, higher bit rate, or long distance transmission.

Compared with mw/m^2 of single channel systems, the high intensity of optical launched power in WDM system raises to Mw/m^2, while also enlarging the fiber nonlinear effects. Inter-channel cross-talks among multiple channels are also increased by the raising bit rate along the transmission links. For dispersion compensation fiber (DCF), the effective core area of DCF is ~20 μm^2which is even smaller than ~80 $\mu m^2$of SSMF. Such a well–confined propagation medium is strongly influenced by impairments.

This chapter briefly introduces the major fiber nonlinearities, alongside exploring their interactions with noise and filtering impacts. In section 3.1, basic nonlinear behaviors in

optical fibers are generally discussed. Further, three major nonlinear impairments including self-phase modulation (SPM) in section 3.2, cross-phase modulation (XPM) in section 3.3, and nonlinear polarization scattering or cross polarization modulation (XPOLM) in section 3.4 are studied. At the end, we focus on phenomena interactions in section 3.5.

3.1 Nonlinear behaviors in fiber-optics

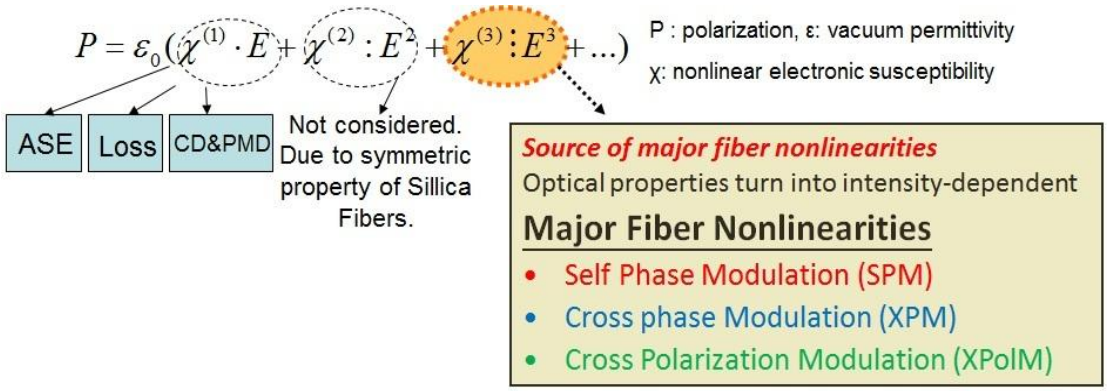

Figure 3.1 Major Nonlinear Impairments

While the intense lights travel along the transmission links, the optical carriers interact with atoms and electric charge. Under the influence of intense electromagnetic fields, the characteristics of the lights in an optical fiber, such as refractive index, polarization, and dielectric constant become dependent on the electrical field E. For instance, this influence turns the polarization into nonlinear, and the polarization must generally be presented in a form of series in which the terms are proportional to different powers of electrical field:

$$P = \varepsilon_0(\chi^{(1)} \cdot E + \chi^{(2)} : E^2 + \chi^{(3)} \vdots E^3 + \ldots)$$

where P is the polarization induced by electric dipoles; εis the vacuum permittivity. In this harmonic function, the first susceptibility represents the linear properties of the optical fiber which are related to refractive index and loss coefficient. These properties can generate several fundamental impairments such as loss, noise, polarization mode dispersion (PMD), and chromatic dispersion (CD). The second susceptibility can be ignored in optical fiber communication system because of the symmetry of SiO2. Moreover, the third order susceptibility is responsible for the nonlinear effects such as self-phase modulation (SPM), cross phase modulation (XPM), and nonlinear polarization scattering (NPS) or cross polarization modulation (XPOLM) [22-24]. The influence from these phenomena was solved by the discovery of highly nonlinear optical fiber, but it becomes significant in the high-capacity long-haul transmission system [25].

3.2 Self-Phase Modulation (SPM)

Self-phase modulation is an important impairment that causes pulse broadening and dispersion in optic fiber communication. According to optical Kerr Effect [26], refractive index varies as a function of optical power which can be described as

$$n_r = n_o + n_2'(P / A_{eff})$$

where P is the power, n_r is the refractive index depending on optical power, n_0 is linear refractive index; A_{eff} is effective core area, and n'_2 is nonlinear coefficient. Overall phase of optical field is the derived as

$$\emptyset = n_r kL = n_0 kL + n'_2 \frac{P(z)}{A_{eff}} kL$$

where L is total fiber length. Thus, nonlinear phase shift can be given by

$$\emptyset_{NL} = n'_2 \frac{P(z)}{A_{eff}} kL = \frac{2\pi}{\lambda} \frac{n'_2}{A_{eff}} \int_0^L P(z)dz = \gamma L_{eff} |E|^2$$

,which is in proportion to intensity. The nonlinear phase shift due to the variation of refractive index is known as self-phase modulation (SPM) [27]. $\gamma = \omega_0 n_2' / A_{eff} c$ is the fiber nonlinear parameter with c as light speed and ω as angular frequency. $L_{eff} = 1 - e^{-\alpha L} / \alpha$ is the effective fiber length with α as fiber loss coefficient.

Through the equation of γ, the nonlinear parameter depends inversely on effective core area and thus, SPM-induced phase shift reduces by increasing A_{eff}. Either the impact created by SPM or cross phase modulation can be decreased with large effective core area fibers. However, in the long-haul optic fiber transmission system, nonlinear phase shift would become significant and turns into nonlinear phase noises due to the low-loss fiber and thus large effective fiber length L_{eff} .

For phase or frequency modulation, the initially constant characteristic of amplitude is a resistance of nonlinear phase nonlinear. Nevertheless, the spontaneous emission noise, caused by the optical amplifiers, produces optical power fluctuations. These power fluctuations create nonlinear phase noises through Kerr Effect [26] and raise the phase fluctuations in the receiver end.

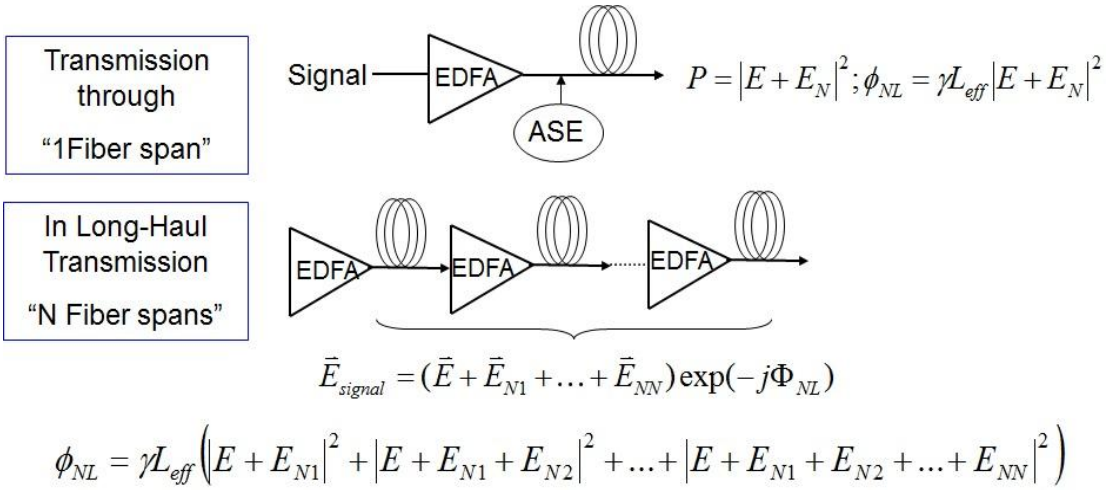

Figure 3.2 Nonlinear phase shift induced by ASE from EDFA

If we assume that the baseband representation of electrical field is E and the baseband representation of ASE noise is n, the nonlinear phase noise is given by

$$\phi_{NL} = \gamma L_{eff} |E + n|^2 = \gamma L_{eff} |E|^2 + 2\gamma L_{eff} \operatorname{Re}\{E \cdot n\} + 2|n|^2$$

where the nonlinear phase noise is caused by SPM and ASE noise. In n-span optical fibers, the nonlinear phase noise can be described as

$$\phi_{NL} = \gamma L_{eff} \left(|E_0 + n_1|^2 + |E_0 + n_1 + n_2|^2 + \ldots + |E_0 + n_1 + n_2 + \ldots + n_N|^2 \right)$$

where E_0 is the baseband representation of electrical field and $n_1 \sim n_N$ are the phase noise created by ASE noise introduced into the system. The impact of nonlinear phase noise produced by self-phase modulation and amplifier spontaneous emission noise is first proposed by J.P. Gordon and L.F. Mollenauer in 1990 [28].

3.3 Cross-Phase Modulation (XPM)

Addressing the issue of WDM crosstalk is crucial for future WDM systems [2, 29, 30]. When one or more optical channels are transmitted simultaneously in the same optical fiber, the power fluctuations are not only effected by one but two or more different channels. Therefore, the nonlinear phase noise due to intensity dependence of refractive index can be in induced from other channels in a multiple channel optic fiber communication system. This phenomenon is known as cross phase modulation (XPM).

Including SPM and XPM, the overall nonlinear phase shift for the jth channel, as shown in Fig.4-1, is given by

$$\phi_j^{NL} = \gamma L_{eff} (P_j + 2\sum_{m \neq j} P_m)$$

where the sum extends over the number of channels. The first term on the right side can be understood as the influence of SPM. The second term is responsible for XPM acquired by other channels. As seen in the equation, the factor "2" indicates that XPM-induced nonlinear effect is twice stronger than SPM-induced nonlinear effects at the same launch power.

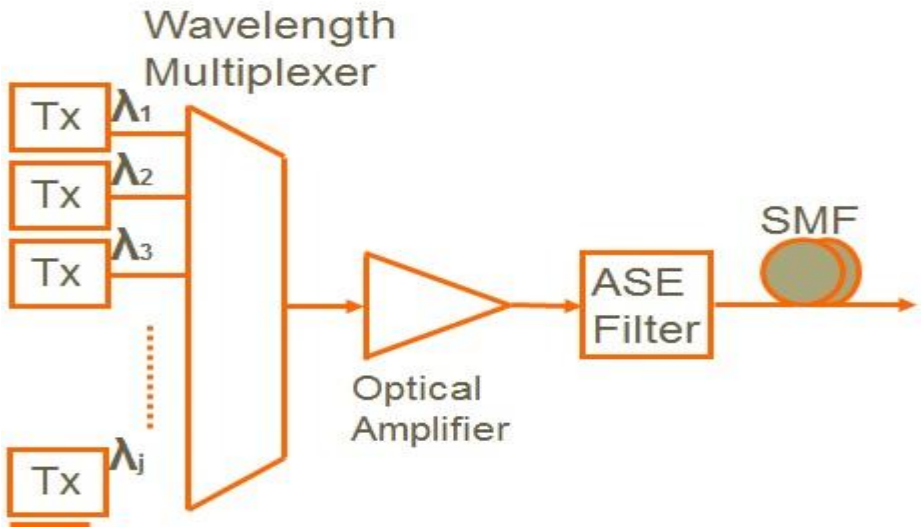

Figure 3.3 Cross Phase Modulation

In practical, because of Walk Off effect, the XPM-induced nonlinear phase shift only occurs when two pulses overlap. On the other hand, if we consider the crosstalk between two widely separated channels and the group velocity dispersion is negligible through using dispersion compensating fibers (DCF), the nonlinear phase shift should not affect system performance. Since the pulses overlap for such a short time in two widely separated channels and less broadening of signal pulses in DCF, the pulses will not overlap enough time for XPM effect to accumulate. Consequently, using neighboring channels and a sort of fibers with smaller effective core area (A_{eff}) in the experiments will be a method to help measure cross phase modulation [22].

3.4 Nonlinear Polarization Scattering

Let's precede an analysis in a Polarization Multiplexing system where two optical channels are transmitted with two orthogonally polarized lights along the fiber. As mentioned in the introduction, fiber birefringence induces polarization mode dispersion

(PMD) which causes pulse broadening and distorts the signal. By using the polarization-maintaining fiber, such fiber will exhibit nearly constant birefringence. This is called linear birefringence. While the nonlinear effects become more important, a nonlinear polarization scattering induced by nonlinear birefringence will start degrading the system performance in polarization multiplexing modulation systems. Similar to cross phase modulation that the nonlinear phase shift caused by one frequency component, nonlinear polarization scattering produced phase shift due to the interaction between two orthogonally polarized carrier waves or between the pump power and each polarization.

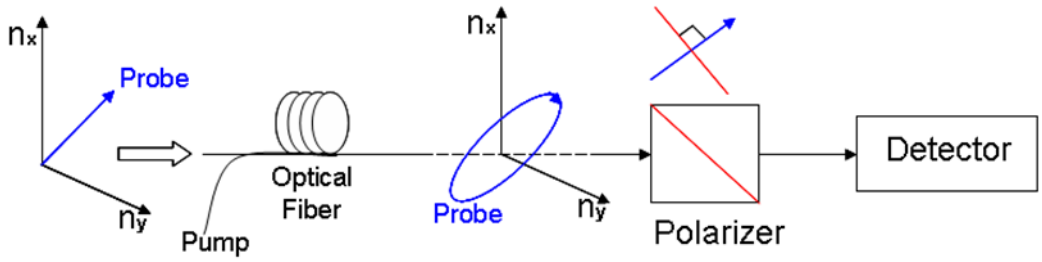

Figure 3.4 Nonlinear Polarization Scattering

The nonlinear polarization scattering can be understood from Figure 3.4, a scheme which is an illustration of Kerr shutter. A probe with two orthogonally polarized lights transmits through an optical fiber. At the output end, a crossed polarizer is placed to block probe transmissions. The power induced by the pump, which has a different wavelength from probe, causes different power fluctuations to the polarizations of the probe. This generates that the refractive indices of parallel and perpendicular polarization components become different. As the polarization components of probe slightly changes after the nonlinear birefringence induced by the pump, a portion of probe power will

transmit through the polarizer. This phenomenon is known as nonlinear polarization scattering.

Chapter 4
Modulation Formats for High Spectral Efficiency

Optical modulation facilitates information transfer through silica fibers, while also determining the characteristics of transmission. Through different modulation formats, electrical signals could be converted into an optical bit stream in intensity or amplitude, frequency, and phase domain. By modulating optical carriers, it is able to enhance system transmission tolerances, while also increasing system capacity. In this chapter we focus the modulation formats deployed in high spectral efficiency optical transmission.

First of all, section 4.1 briefly introduces on-off keying that is widely used for terrestrial optical fiber transmission. Continuously, differential phase shift keying (DPSK) will be discussed in section 4.2. In section 4.3, we focus on optical duobinary, a widely used optical modulation formats in 40Gb/s transmission systems. Section 4.4 presents differential quadrature phase shift keying (DQPSK). At the end, we describe polarization multiplexing technique in section 4.5.

4.1 On-Off Keying

On-Off keying (OOK) modulation format converts the information onto optical carriers over the amplitude of light, which can also be realized as switching the output of optical power ON and OFF mapping binary electrical bits 0 and 1. OOK can be classified to

Non-return-to-zero (NRZ) OOK and return-to-zero (RZ) OOK according to signal pulse shapes. Figure 4.1 describes NRZ- and RZ- OOK formats, where the difference between NRZ and RZ is depending on the occupation of a signal pulse during a bit period. For NRZ, a signal state, 1 or 0, occupies the whole time length of bit period. In RZ format, less than a bit period of signal state is occupied.

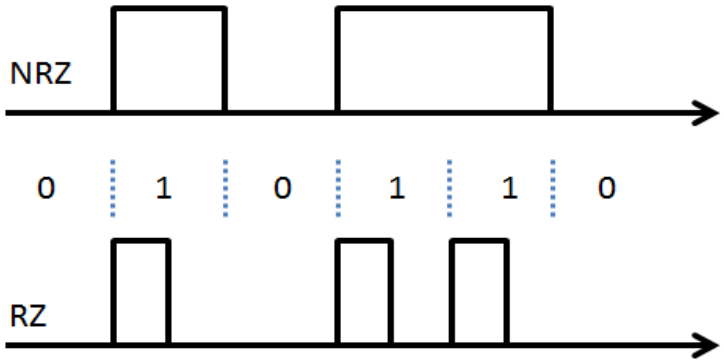

Figure 4.1 RZ and NRZ signal

NRZ-OOK has been widely used for commercial applications for 10 Gb/s intensity modulation system, where both direct and external modulation can be used for transmitters. However, for long-haul transmissions, less residual chirp makes external modulation more attractive in comparison to direct modulation. External modulation in use of Mach-Zehnder modulator (MZM) modulating the output of distributed feedback laser (DFB) is typically employed for NRZ-OOK system. **Error! Reference source not ound.** shows the operation of a NRZ-OOK transmitter with a MZM. The MZM is driven by the electrical signal with required swing voltage equal of V_π at quadrature point of the transmission curve. Thus, the intensity of high and low is corresponding to the electrical voltage of V_π and 0.

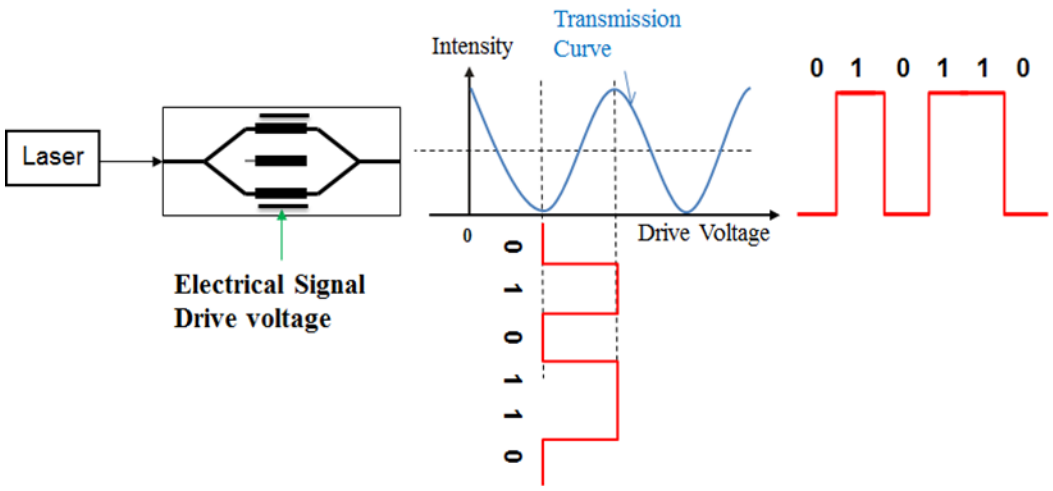

Figure 4.2 NRZ-OOK modulation

Because 1-to-0 or 0-to-1 transitions happen fewer times, NRZ has smaller bit stream and needs roughly half the bandwidth of RZ. Meanwhile, RZ needs more precise control of pulse width so less inter-symbol interference (ISI) occurs in RZ format. Compared with NRZ pulses, RZ pulses also benefit from a soliton-like effect in optical fiber and suffer less distortion due to fiber nonlinearity. Therefore, RZ attract most attention in the ultra-long haul submarine systems but NRZ is typically used in terrestrial transmission system

4.2 DPSK

Differential phase shift keying (DPSK) like PSK is based on utilization of phase, but DPSK uses phase changes between two symbols of an optical carrier to carry the information. As shown in **Error! Reference source not found.**, a NRZ-DPSK ransmitter usually consists of a MZM with bias voltage of $2V_\pi$ driven at minimum point of the transmission curve. The swing voltage (V_π, $-V_\pi$) are mapping onto two phase states with the same energy level. Through measured eye diagram after the transmitter, it

is clear to realize that two levels of intensity correspond to phase difference of π and 0, respectively. DPSK system has an obvious benefit of ~3dB lower OSNR for receiver sensitivity because of $2V_\pi$ drive voltage. The lower OSNR requirement can extend the transmission distance, reduce optical power requirements, and relax component specifications[31].

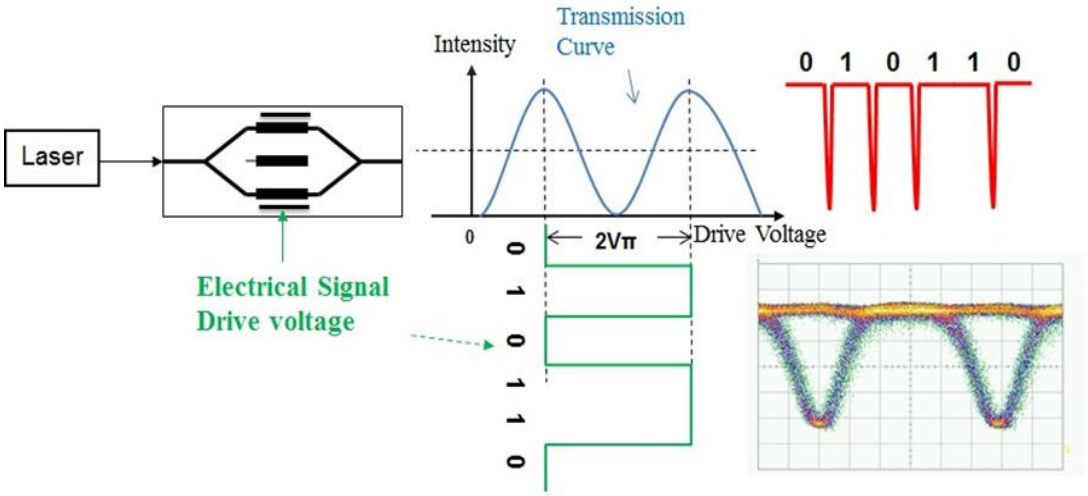

Figure 4.3 Structure of DPSK transmitter

4.3 Duobinary

Duobinary modulation also known as partial response was originally introduced in 1960's by Lender as a more efficient format with alternative advantages compared with pulse amplitude modulation [32]. The main transmission intelligence of duobinary is modulating certain correlation characteristic between consecutive bits [33]. In 1980, the first optical duobinary experiment using as a 3-level amplitude modulation is demonstrated. Duobinary modulation was originally conceived as a more efficient format compared with binary pulse amplitude modulation (PAM) for transmitting high-speed

electrical signals over bandwidth limited channel. In fiber-optic communications, duobinary modulation has also stimulated much interest, especially as a practical alternative for high-spectral efficiency 40 Gb/s systems [34-37], alongside the more popular differential phase shift keying (DPSK) technique [31]. Both duobinary and DPSK can achieve the high spectral efficiency necessary to transmit 40 Gb/s data on a 50 GHz channel spacing, albeit with different engineering tradeoffs [38-40].

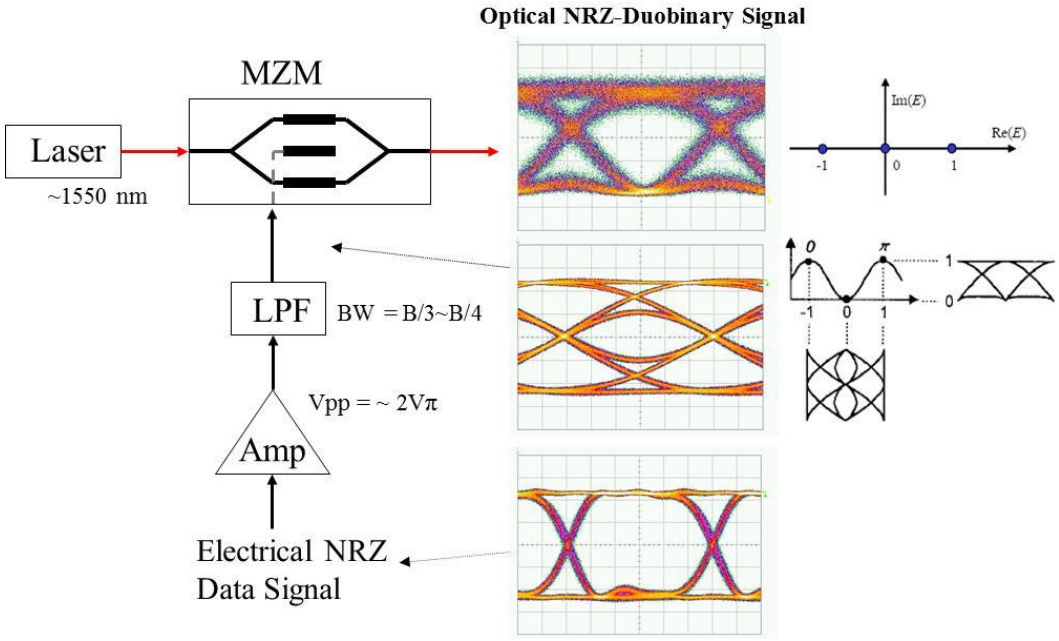

Figure 4.4 Structure of Duobinary Transmitter

As displayed in Figure 4.4, an optical NRZ-duobinary signal can be generated by driving a LPF-filtered electrical signal on a MZM. The electrical NRZ signal is converted into a 3-level with swing voltage of V_{pp} equal to $2V_{\pi}$ by a duobinary generated LPF. The bandwidth of LPF is typically 28% of bitrate, and a wider 40% of bitrate. Optical duobinary has stimulated a lot of interest especially for 40 Gb/s optical transmission

system. Optical duobinary is a spectrally efficient modulation format in limited channel spacing due to the more compact pulse shape, which also increases the tolerance to the chromatic dispersion.

4.4 DQPSK

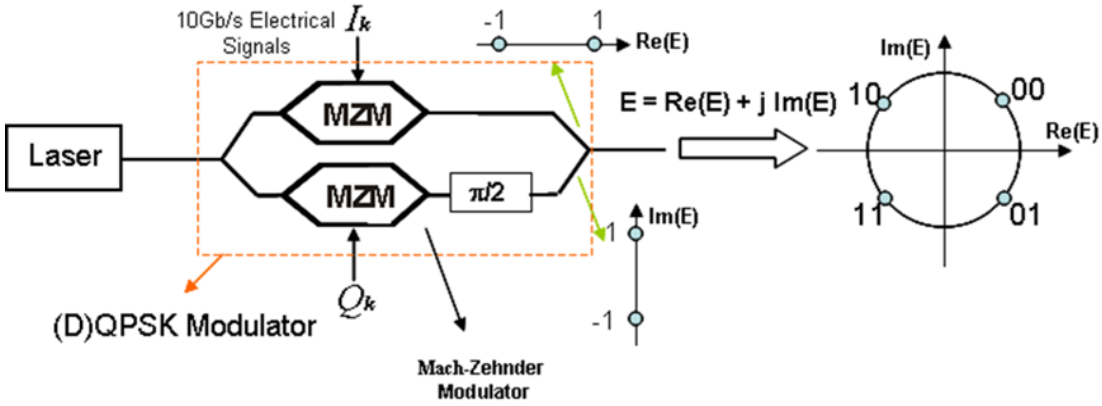

Figure 4.5 Structure of DQPSK transmitter

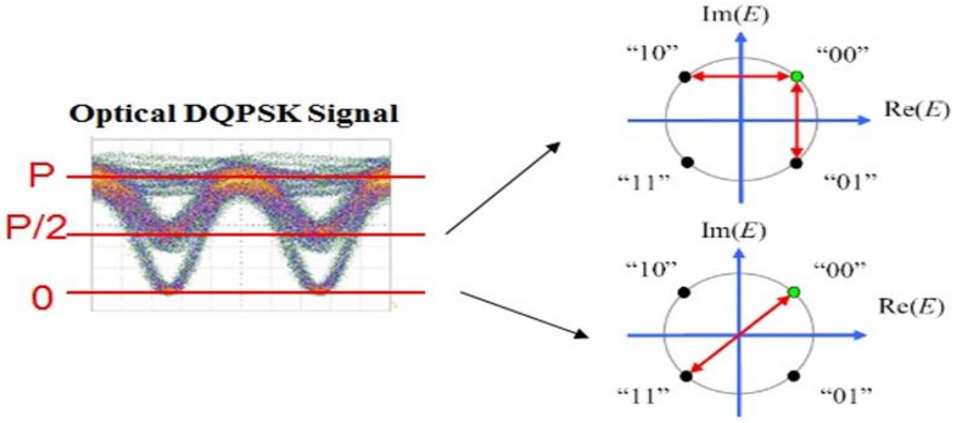

Figure 4.6 Eye diagrams of DQPSK

Advanced multilevel modulation is a key component for enabling high-spectral efficiency transmission of optical fiber communication. Differential quadrature phase-shift keying (DQPSK) is one of the multilevel modulations that are able to achieve 2X spectral efficiency of intensity modulation. Thus, DQPSK has received considerable attention recently [30, 41, 42]. In DQPSK optical transmission systems, the information data sequence is converted into four different phase states of optical carriers, and the transmitted signal will be demodulated through the phase difference between consecutive bits. Figure 4.5 demonstrates the structure of DQPSK modulator with a constellation of 4 phase states. The light split into two MZMs which are driven by the electrical signals of data sequence I_k and Q_k separately, thus both branches of optical carriers are converted into two DPSK optical signals. As seen on the constellation in Figure 4.5, the in-phase optical carrier of $Q_k$is able to be transferred into quadrature phase signals by phase shifter of $\pi/2$. The upper branch will be mapped into [-1, 1] (or 0 and π) at real axis and the lower branch with phase shifted by $\pi/2$ represents [+j, -j].

In DQPSK systems, all the information can be encoded into four possible phase changes. As can be clearly seen in , similar to DPSK eye diagrams, DPSK eyes consists of two dips of energy levels, P and P/2, each of which corresponds to different phase shifts on the constellation.

In Table 4-1, each set of data bits is encoded into one phase change. Each phase change can be demodulated naturally through DQPSK modulator. Thus, it is able to reduce bandwidth requirement for both transmitter and receiver symbol rate is in use of half bit

rate which reduces bandwidth requirements for the transmitter and receiver. One path of DQPSK modulator converses bits to 1,-1 and another path converses bits to j, -j. The combined output field equals to $E_o = \mathrm{Re(E)} + \mathrm{jIm(E)}$ resulting symbols within [1+j, 1-j, -1+j, -1-j] which maps onto [$\frac{\pi}{4}, \frac{3\pi}{4}, \frac{5\pi}{4}, \frac{7\pi}{4}$].

Data bits	Optical Field	Phase State	Phase Change
00	1 + j	π/4	0
01	1 - j	7π/4	3π/2
10	-1+ j	3π/4	π/2
11	-1 – j	5π/4	π

Table 4-1

4.5 Polarization Division Multiplexing

So far, utilizations of amplitude, phase, and frequency for modulations have already been discussed in previous sections. In addition to the use of these three characteristics of light, a different approach to increase system capacity is the application of polarization. Polarization-Division Multiplexing (PDM), sometimes also called polarization-multiplexed modulation (Polmux) or dual-polarization (DP), is the utilization of two orthogonal polarization states, slow and fast axis, to transmit two different data sequences, respectively. As presented in **Error! Reference source not found.**, the information data

re modulated onto optical carriers at the transmitters both operating at the same wavelength but orthogonal polarization states. The combined optical carriers are able to transmit double information data with the same symbol rate. For instance, a Polmux-DQPSK system, which was used for 2.56-Tb/s transmission in a single channel [43], is able to increase the transferred bitrate by a factor of 2 in comparison to single DQPSK system.

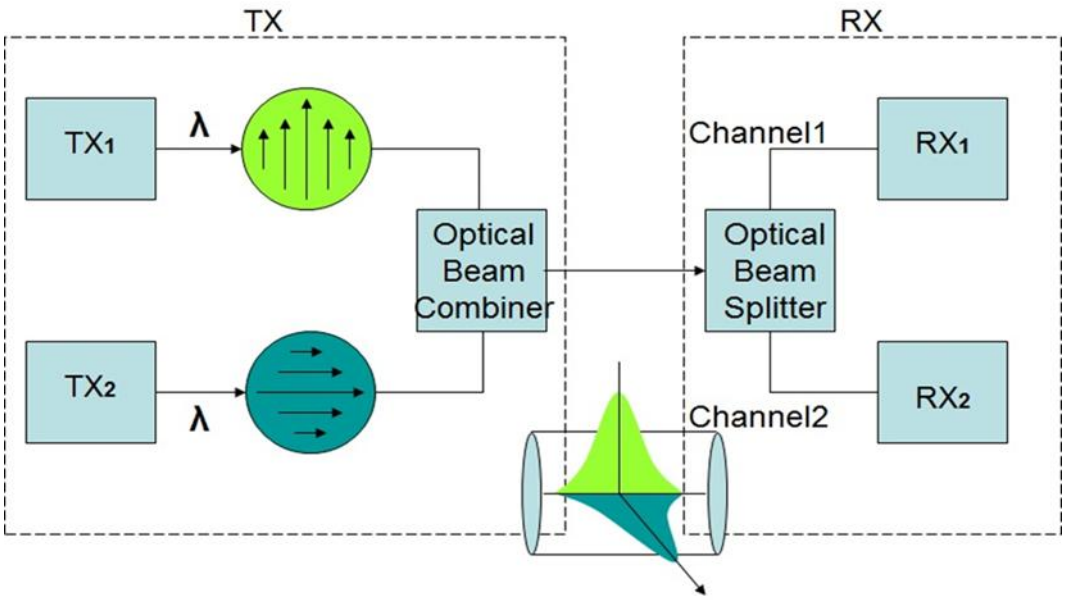

Figure 4.7 Introduction of Polarization Multiplexing Division

However, modulation in use of Polmux only draws modest attentions due to the requirement to sensitivity of polarization at the receiver. Due to fiber birefringence in optical fibers, polarization becomes time dependent along the transmission links. A Polmux transmission system also requires a more complicated receiver for polarization demultiplexing, compared with single-polarization modulation system. Instead of

complicity, linear and nonlinear transmission tolerance can be reduced by applying Polmux signaling. The double spectral efficiency of Polmux system is able to compact the spectral width, alongside being more tolerant to chromatic dispersion but with lower required OSNR. In the following chapters, we include the experimental results of linear and nonlinear tolerance for Polmux-DQPSK systems. For 100G DP-QPSK simulations, the tolerance to nonlinear impairment is also analyzed.

Chapter 5
Balanced Detection Schemes for Duobinary

In previous chapter, we focused on different types of high spectral efficiency modulation formats, where section 4.3 briefly introduces optical duobinary modulation format. In this chapter, we discuss in more details on the properties of optical Duobinary through a 10-Gb/ system experimentally and 40-Gb/s system simulatedly. Typically, DPSK has obtained more favor due to the advantage of OSNR sensitivity, compared with optical duobinary. However, most studies have taken consideration of optical duobinary with direct detection but not with balanced detection. The following study will demonstrates that balanced detection is a more suitable for duobinary in both linear and nonlinear regime, while also showing our proposed receiver. As both Duobinary and DPSK share some interesting connections, DPSK is also added for references in this chapter. In particular, balanced detections including our proposed receiver are focused here in both linear and nonlinear regimes.

In fiber-optic communications, duobinary modulation has stimulated much interest of being a practical alternative for high-spectral efficiency 40 Gb/s systems, while also being famed for its good tolerance to chromatic dispersion (CD) and narrow optical filtering. DPSK is also popular for high spectral efficiency long-haul transmission due to the better OSNR sensitivity. Both duobinary and DPSK are able to transmit 40-Gb/s data

on a 50 GHz channel spacing, albeit with different engineering tradeoffs. However, some interesting connections can be found between duobinary and DPSK. For instance, DPSK is able to be converted into duobinary through narrow filtering. Thus, we can consider duobinary as a narrow filtered DPSK. Another interesting connection between duobinary and DPSK is that both output ports of the DPSK delay-interferometer (DI) demodulator produce partial response signals: the DI constructive port converts DPSK into a conventional duobinary signal, while the DI destructive port produces an alternate-mark inversion (AMI) signal.

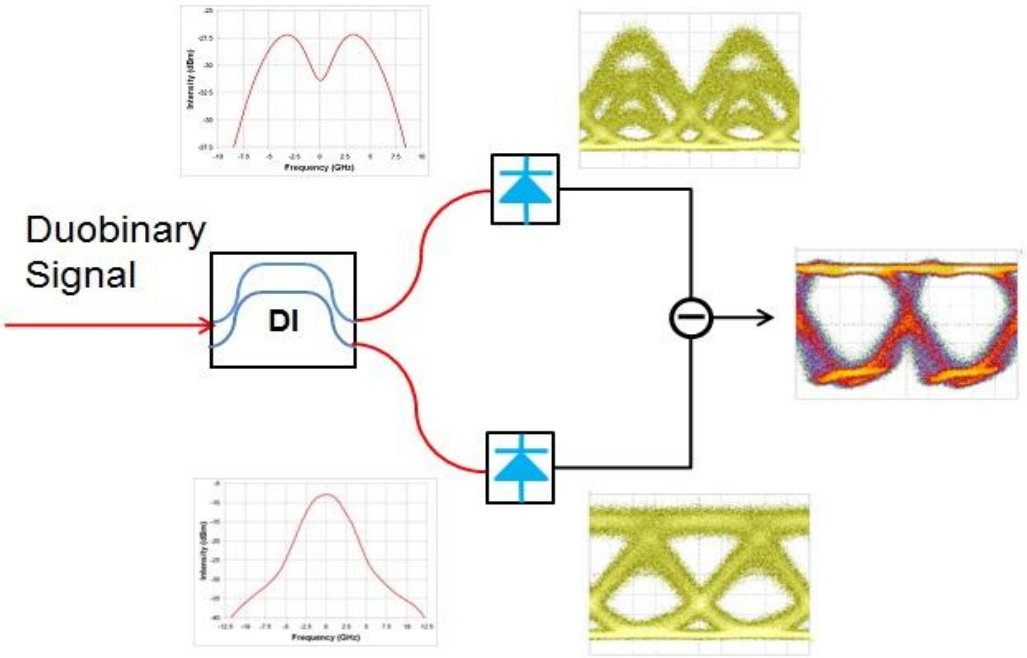

Figure 5.1 Schematic diagram of conventional balanced detection with experimental optical eyes and spectra.

Figure 5.1 shows the measured spectra and eye diagrams for a LPF generated duobinary signal detected using a delay interferometer (DI) and balanced detection. As seen in Figure 5.1, the DI operating on the received duobinary signal produces a distorted version

of an AMI signal component at the top "destructive interference" output port, and a filtered duobinary signal component at the bottom "constructive interference" output port. The duobinary and AMI signal components of DPSK are both necessary to achieve the good OSNR sensitivity using balanced detection. In the case of duobinary, the DI is effectively operating on a narrow filtered DPSK signal, thus producing a highly distorted AMI component. However, despite the distorted nature of the reconstructed AMI signal component, we demonstrate below using both experiments and simulations that the balanced receiver yields a significant advantage for duobinary systems.

5.1 Experimental Results and Analysis

5.1.1 Experimental Setup

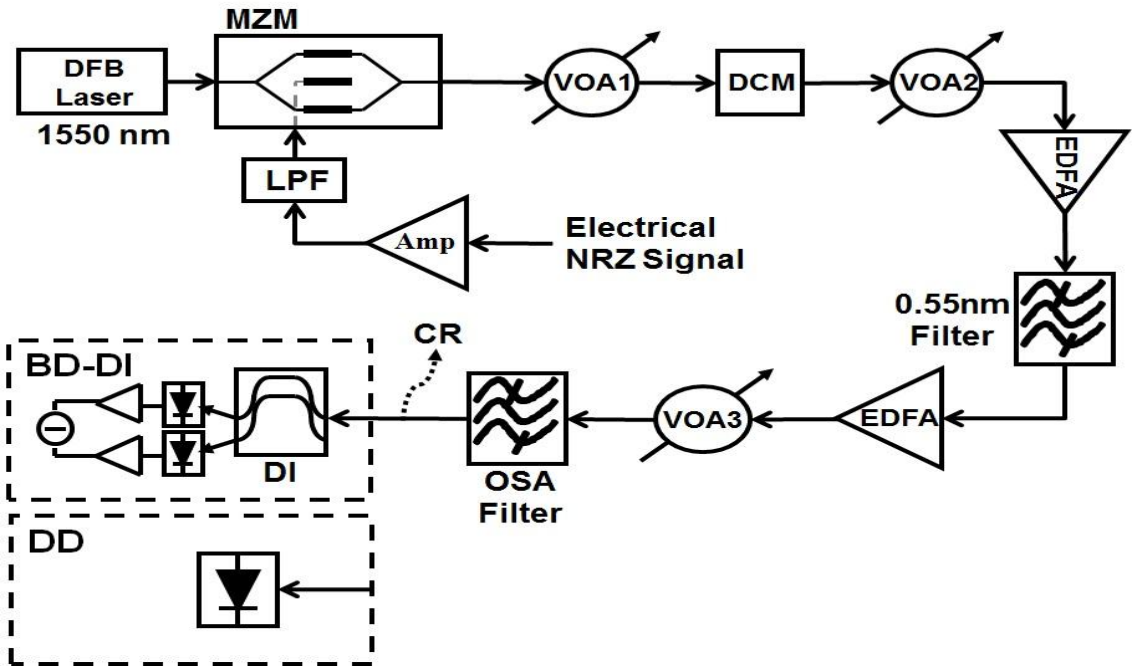

Figure 5.2: Experimental setup for testing 10 Gb/s duobinary and DPSK systems.

Figure 5.2 shows the experimental setup for testing 10 Gb/s NRZ-duobinary and DPSK systems with both direct and balanced detection receivers. The optical carrier wave at 1550 nm emitted by a distributed feedback (DFB) laser is modulated by a Mach-Zehnder modulator (MZM). To produce an optical duobinary signal, the MZM is biased at a null, and driven with an electrical duobinary signal amplified to $\sim 2V\pi$. The electrical duobinary signal is generated by passing a pseudo random bit sequences (PRBS) of length 2^{15}-1 from pulse-pattern generator (PPG) through a duobinary generating low-pass filter (LPF). The duobinary LPF bandwidth is optimized as discussed below. For varying LPF filter bandwidth, we employ different bandwidth Bessel–Thomson-type filters obtained from the same manufacturer.

The duobinary generating LPF is removed for testing DPSK systems. Note that while differential pre-coding is necessary in practice for both duobinary and DPSK systems, it is not necessary in experimental systems using PRBS data. The transmitter output power is controlled using a variable optical attenuator (VOA1). The optical signal is then optionally launched into a dispersion compensating module (DCM) of -1100ps/nm for evaluating the influence of chromatic dispersion, or launched directly into VOA2, which controls the input power into an optically pre-amplified receiver, for back-to-back (B2B) measurements.

As seen in Figure 5.2, the optically pre-amplified receiver employed a two-stage EDFA design with a 0.55 nm optical filter placed in the middle to minimize the amplified spontaneous emission (ASE) noise input to the second stage. An optical spectrum

analyzer (OSA) placed at output of the second EDFA stage, and operating in a WDM filter mode, is used as a tunable bandwidth optical filter to test the impact of optical bandwidth [44]. The optical bandwidth is set by tuning the OSA resolution (e.g. 0.2 nm OSA resolution corresponds to a measured FWHM bandwidth of 23.2 GHz). For direct detection, the typical detection mode used in duobinary systems, we employ a commercial PIN photodetector with a 9 GHz electrical bandwidth. For interferometric balanced detection, we tested a DI with free-spectral range (FSR) equal to the bitrate or 10 GHz, as well as a DI with a wider FSR equal to 12 GHz for comparison. A balanced receiver with DI FSR greater than the bitrate is interesting for duobinary because such a configuration was shown to give better tolerance to narrow optical filtering in DPSK systems [45], and duobinary can be considered as an extreme case of a narrow filtered DPSK. The input average optical power into the DI is controlled by VOA3 to be fixed at -6.5 dBm. The balanced receiver includes an integrated LA, and is specified to have an electrical bandwidth of 20 GHz. Clock recovery (not shown in Figure 5.2) is achieved by taping a portion of the optical signal at output of OSA filter into a separate DPSK or OOK receiver which includes a clock-recovery circuit.

5.1.2 Experimental Spectra

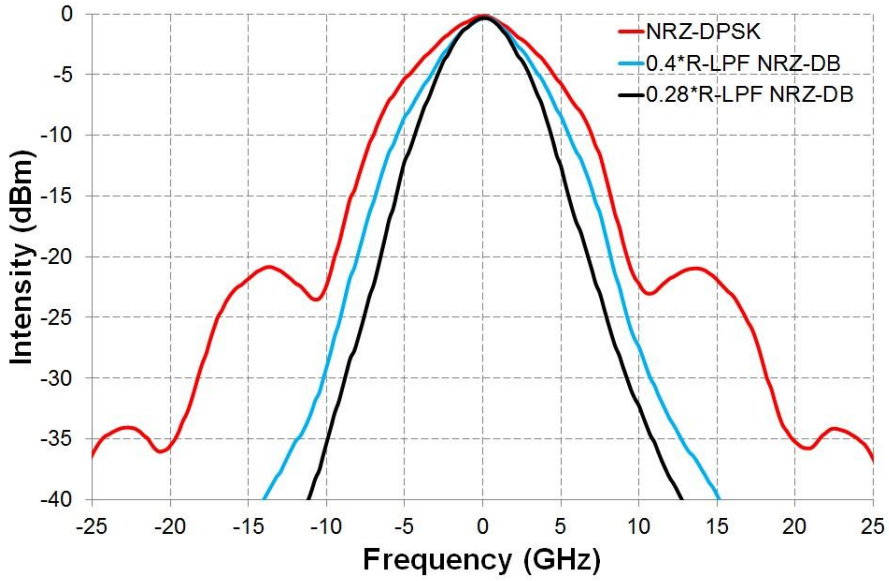

Figure 5.3 Comparison of three measured optical spectra at 10Gb/s. The OSA resolution is 0.01 nm.

The measured 10 Gb/s optical signal spectra in our experiment are compared in Figure 5.3 for NRZ-DPSK, and duobinary (DB) with LPF bandwidth equal to the standard value 28% of bitrate, as well as a wider LPF bandwidth 40% of bitrate. As is well known, the duobinary signal exhibits a more compact spectrum compared with DPSK, which is advantageous for achieving the Nyquist limit of spectral efficiency, as well as for improved tolerance to optical filtering, WDM crosstalk, and chromatic dispersion. Of course, it is possible to convert a DPSK signal into duobinary using narrow optical filtering, which blurs the definition of a duobinary signal. However, we believe a LPF generated duobinary signal, also known as Phase Shaped Binary Transmission (PSBT), is a distinct modulation format [46-49]. Certainly there are advantages to generating a duobinary signal in electrical domain using the LPF technique, e.g. effectively reducing

the bandwidth requirements on the modulator by a factor of 2-4 compared with DPSK [49, 50]. Also, when using narrow optical filtering to convert DPSK into duobinary, any drift of the narrow optical filter from the ITU grid would induce severe signal distortion. This problem is avoided in LPF-generated duobinary. The LPF generated duobinary with LPF bandwidth equal to ~ 40% of bitrate is also a special and interesting case, where the generated signal is a kind of hybrid between duobinary and DPSK. As shown below, this duobinary generating LPF design gives an excellent performance when combined with balanced detection.

5.2 Experimental Results and Analysis

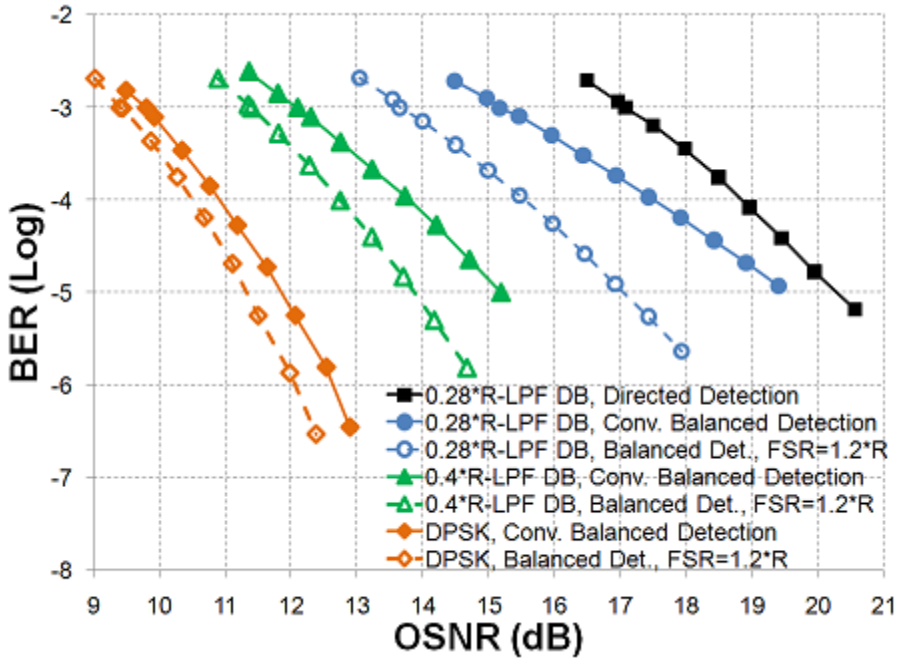

Figure 5.4 B2B measured receiver sensitivity for direct detection and balanced detections in duobinary and DPSK systems.

Figure 5.4 reports the measured back-to-back (B2B) BER as a function of OSNR for duobinary and DPSK systems based on various detection schemes. The OSNR controlled by VOA2 is measured at the output of first EDFA stage in Figure 5.2 before the 0.55 nm optical filter; the second EDFA stage has a negligible impact on the received OSNR since the mid-stage loss of the 0.55 nm optical filter is much smaller than the EDFA gain.

The OSA optical receiver filter at output of second stage EDFA is fixed at 0.2 nm resolution or an optical bandwidth equal to 23.2 GHz. The data in Figure 5.4 demonstrate that balanced detection gives a significant advantage over direct detection for conventional 0.28*R-LPF duobinary. As expected, the DI with wider FSR = 1.2*R gives the most gain in performance for duobinary, more than 4 dB at BER = 10^{-3}. Our data show that an even better result can be achieved for duobinary with balanced detection when the LPF is designed to have a wider 0.4*R bandwidth. In this case, with DI FSR=1.2*R, duobinary gains more than 6 dB using balanced detection compared with direct detection. This duobinary performance approaches to within ~ 1.5 dB of DPSK in our experiment. We believe this is a remarkable result, considering that receiver sensitivity is typically not considered to be a strong point of duobinary modulation.

As implied in the measurement results above in Figure 5.4, the duobinary generating LPF is a key element for optimizing the duobinary system. To ensure a fair comparison between balanced detection and direct detection, we conducted B2B measurements of required OSNR (ROSNR) versus LPF bandwidth. As in the experiment of Figure 5.2, the receiver optical filter bandwidth was fixed at 23.2 GHz. Figure 5.5 shows the measured ROSNR for BER=10^{-3} as a function of LPF bandwidth for duobinary based on direct

detection, balanced detection with DI FSR bandwidth equal to R, and FSR bandwidth equal to 1.2*R. The data in Figure 5.5clearly demonstrate the advantage of balanced detection over direct detection for duobinary through the entire range of LPF bandwidths tested in the experiment. Another clear trend shown in Figure 5.5 is the benefit of using a DI with FSR greater than the bitrate, especially for the narrowest LPF bandwidths. The performance gain of balanced detection for duobinary increases with LPF bandwidth, approaching the DPSK performance. The tradeoff in increasing LPF bandwidth is a wider signal spectrum, also approaching the DPSK spectrum.

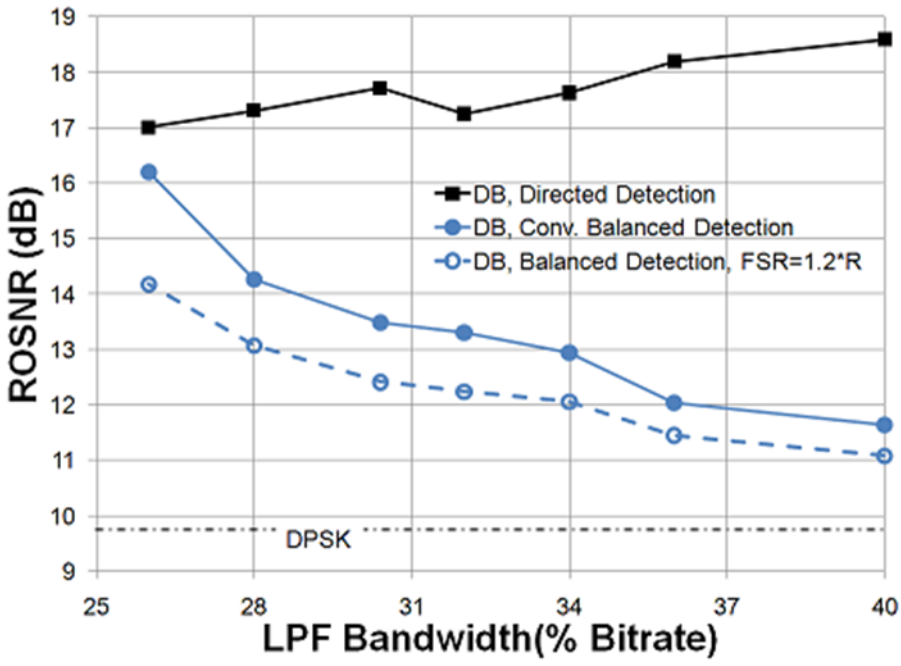

Figure 5.5 B2B measured Required OSNR (ROSNR) versus LPF bandwidth.

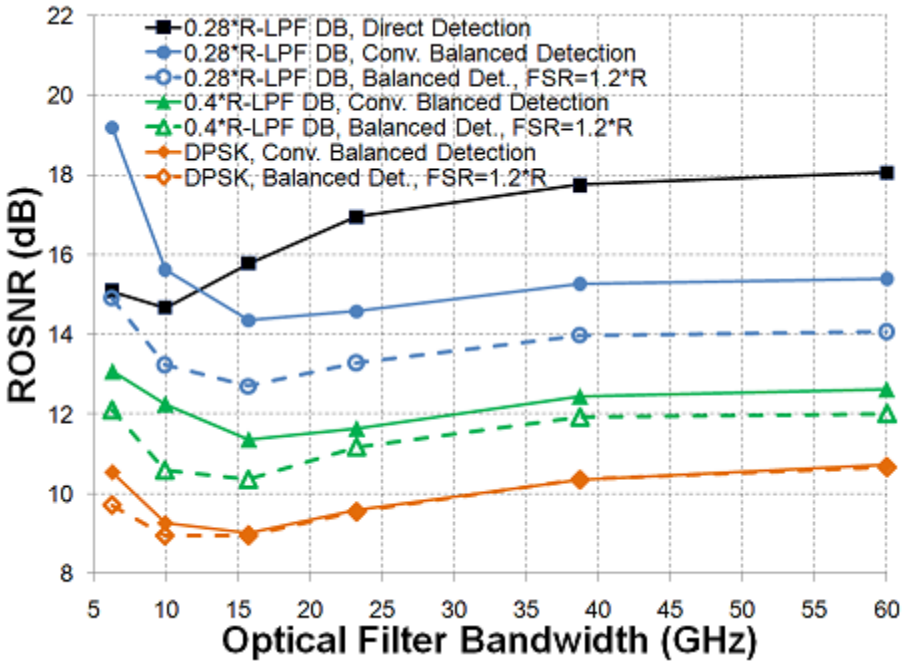

Figure 5.6 B2B measured ROSNR as a function of optical filter bandwidth. Dashed curves correspond to balanced detection with DI FSR = 1.2*R.

It is also interesting to study the impact of optical filtering on the various detection schemes. Figure 5.6 shows the measured ROSNR versus receiver optical filter bandwidth. The LPF bandwidth is chosen to be 28%, 40%, or 100% (DPSK) of bitrate. In conventional 0.28*R-LPF duobinary modulation, the optimal optical filter bandwidth occurs at ~ 10 GHz for direct detection compared with ~ 15.7 GHz for balanced detection. This difference can be explained in the action of DI as an additional "narrow filter" in the balanced detection. Indeed, all the balanced detection schemes tested in Figure 5.6 show about the same optimum receiver optical filter bandwidth, with the wider DI FSR schemes tending to slightly narrower bandwidths. The data in Figure 5.6 confirms that balanced detection is still the preferred detection scheme for duobinary even when receiver optical bandwidths are optimized, as long as the duobinary generating filter and

DI FSR are designed correctly. Figure 5.6 also confirms that duobinary modulation with LPF bandwidth equal to 0.4*R approaches to within 1-2 dB of DPSK at the whole tested range of optical filter bandwidths.

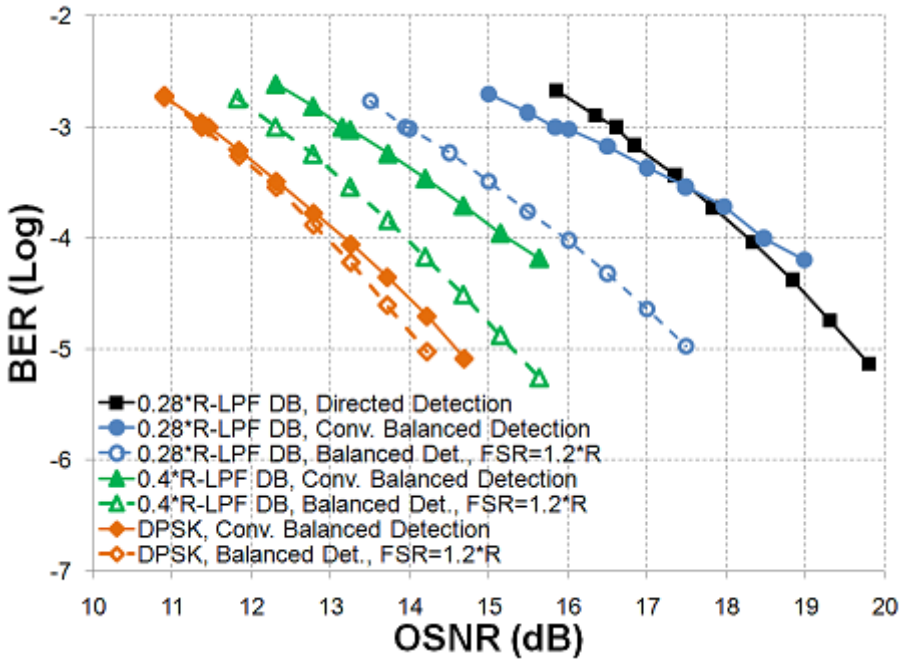

Figure 5.7 Measured Receiver sensitivity including -1100 ps/nm of dispersion.

So far, we have only considered the case of B2B performance, but duobinary could draw more interest in the presence of chromatic dispersion (CD) combined with FSR optimizations. Figure 5.7 reports the measured receiver sensitivity including a dispersion compensation module of -1100 ps/nm dispersion. The receiver optical filter bandwidth is still fixed at 23.2 GHz. With the addition of this modest amount of chromatic dispersion for 10 Gb/s, the duobinary performance approaches closer to that of DPSK. Indeed, the 0.4*R-LPF duobinary with balanced detection and DI FSR=1.2*R reaches to within ~ 1 dB of DPSK at a BER = 10^{-3}. It is also interesting to note that with the influence of

chromatic dispersion, the wider bandwidth DI of FSR=1.2*R has a greater impact on the performance improvement of duobinary with balanced detection. This phenomenon has been observed in recent studies of optimum DI FSR design for DPSK systems [45, 51, 52].

Our experimental setup limits the study of balanced detection schemes for duobinary to 10 Gb/s systems. However, the duobinary advantage in spectral efficiency is especially interesting for higher bitrate 40 Gb/s systems, which we investigate below using computer simulations.

5.3 Simulation Model

To assess the transmission performance of 40 Gb/s duobinary systems based on balanced detection, we carried out detailed Monte-Carlo system simulations at 42.7 Gb/s using the Rsoft commercial simulator OptSim. The simulation model assumes a low-pass filter (LPF) generated duobinary transmitter [51], which is based on a Mach-Zehnder modulator (MZM) biased at a null, and driven by low-pass filtered binary data. We employ a long PRBS 2^{17}-1 data sequence to ensure reliable statistics for Monte-Carlo error counting at a BER = 10^{-3}. The optical multiplexing and de-multiplexing filters are modelled as 3rd order super Gaussian filters with a full-width half maximum (FWHM) bandwidth of 43 GHz to emulate typical terminal equipment for WDM systems operating at 50 GHz channel spacing. ASE noise is added between the two optical filters. At the receiver, we compare direct detection, conventional balanced detection (i.e. using both the constructive and destructive outputs of DI), and the proposed novel balanced

detection scheme, which we call *partially interferometric balanced detection* to emphasize the important feature of only using a DI to generate the AMI signal component. The importance of this feature for duobinary balanced detection will become apparent below. Receiver electrical bandwidth is fixed at 70% of bitrate, and the electrical LPFs used at both transmitter and receiver are modelled as 4^{th} order Bessel filters.

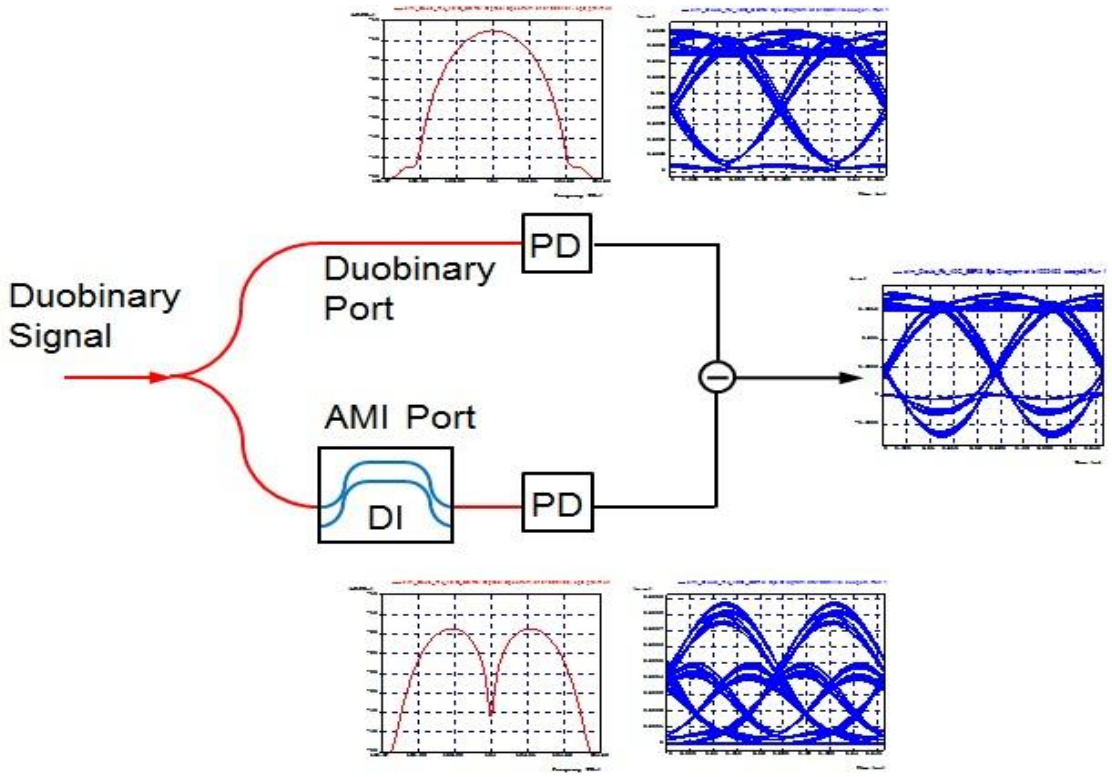

Figure 5.8 Schematic diagram for the proposed duobinary balanced receiver, including simulated signal spectra and eye diagrams.

In an optical duobinary communication system, we essentially have the duobinary component available for the balanced receiver. Indeed, when operating on a duobinary signal with DI, the constructive "duobinary" output port produces an "over-filtered"

duobinary signal, which may degrade performance. This begs the question: can we do better with balanced detection for duobinary by using the DI to only reconstruct the AMI component from the duobinary (i.e. strongly filtered DPSK) signal? This concept is illustrated in **Error! Reference source not found.**, which shows our proposed improved alanced detection scheme for duobinary modulation. After WDM demultiplexing at the receiver, the duobinary signal is split into two branches. The top branch is a copy of the received duobinary signal; it is analogous to the "duobinary port" of the DPSK DI demodulator. The bottom branch includes a DI with delay equal to a bit period, which is used to extract an AMI component from the received duobinary signal; it is analogous to the "AMI port" of the DPSK DI demodulator. Note that since the DI operates on a duobinary signal rather than a clean DPSK signal, it generates a highly distorted AMI component, as can be seen both in experimental eye diagrams of Fig. 1and in the simulated eye diagrams of **Error! Reference source not found.**. However, our imulations confirm that even with a distorted AMI signal component, balanced detection shows a significant advantage over direct detection for duobinary. The simulated optical spectra of duobinary and DPSK transmitters are displayed in Figure 5.9. In both simulated and experimental spectra, the optical duobinary shows the most compact signal spectra in comparison with DPSK.

The simulated optical spectra of duobinary and DPSK transmitters are displayed in Figure 5.9. In both simulated and experimental spectra, the optical duobinary shows the most compact signal spectra in comparison with DPSK.

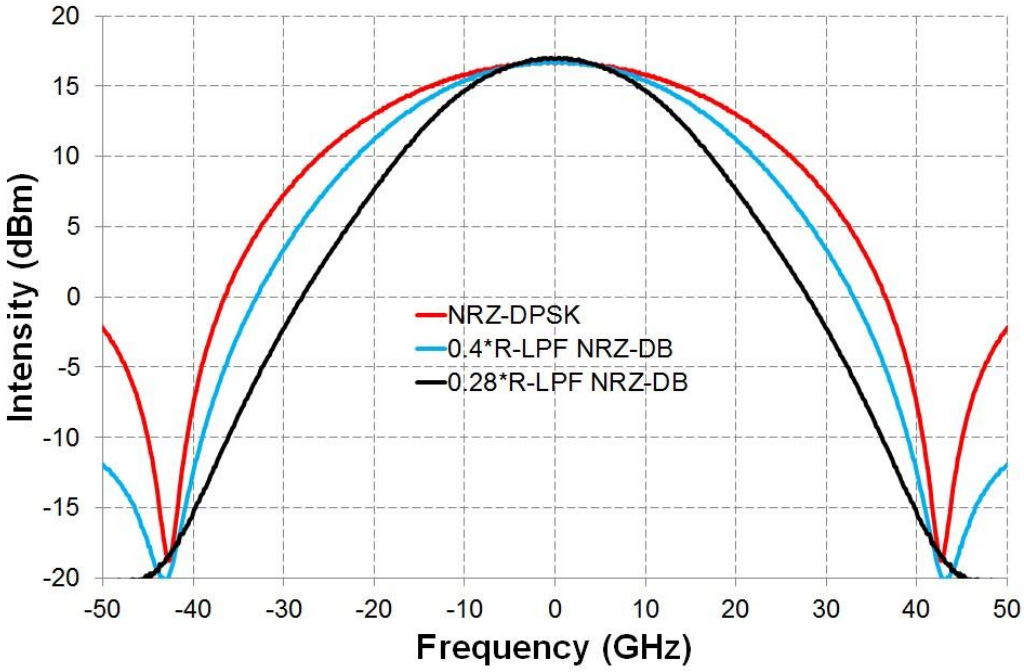

Figure 5.9 Comparison of 42.7 Gb/ simulated optical spectra at output of optical modulator.

5.4 Simulation Results and Analysis

5.4.1 Linear Regime

Error! Reference source not found. shows the simulated ROSNR for BER = 10^{-3} as a unction of duobinary generating LPF bandwidth. Duobinary based on direct detection (squares) follows the typical trend, achieving an optimum performance at a LPF bandwidth ~ 26% of bitrate. Similarly to our experimental results at 10 Gb/s, **Error! eference source not found.** shows that balanced detection offers a significant advantage over direct detection for 42.7 Gb/s duobinary systems with narrow optical filtering, especially when using DI with an FSR = 1.2*R. This advantage induced by balanced detection expands with increasing LPF bandwidth, ultimately admitting duobinary to

approach DPSK performance when LPF bandwidth approximates the bitrate. While the proposed partially interferometric balanced detection (PI-BD) scheme is not the optimal choice for typical duobinary LPF bandwidths, it gives the best performance in the limit of very narrow LPF bandwidths because the "duobinary port" of the PI-BD does not suffer from over-filtering by a DI. This aspect of the PI-DB scheme is particularly useful in fiber networks that include many optical add-drop multiplexing (OADM) filters along the transmission line which may significantly narrow the effective bandwidth.

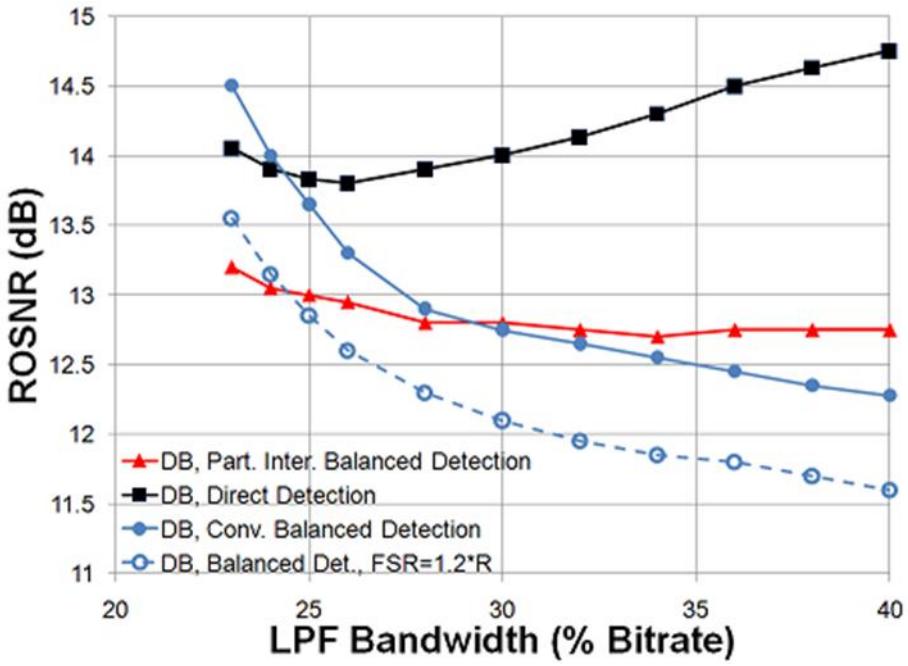

Figure 5.10 Simulated required OSNR versus duobinary generating LPF bandwidth.

The impact of optical bandwidth narrowing due to the presence of OADMs in the optical line system is considered in **Error! Reference source not found.**, where the duobinary enerating LPF bandwidth is fixed at 26% of bitrate (note the simulated spectra and eye diagrams shown in Fig. 8 correspond to this case). The penalty due to OADM cascades

depends on where the ASE noise is added in relation to the optical filtering. In the model of 5.3, the optical carriers pass through cascaded N/2 filters, ASE noise adding EDFA, and then additional cascaded N/2 filters. So for example, N = 2 corresponds to point-to-point (P2P) transmission, while N = 12 includes the impact of 5 OADMs. The simulation results in Figure 5.11 confirm the well-known fact that duobinary with direct detection has an excellent tolerance to tight optical filtering. Indeed, duobinary performance initially improves up to 6 optical filter cascades before gradually degrading back to the P2P performance at ~ 14 filter cascades. Duobinary based on balanced detection with FSR=R shows a poor tolerance to tight optical filtering; ROSNR increases rapidly with filter cascades due to over filtering by the DI. This is also the case for DPSK. In contrast, the PI-BD shows roughly the same tolerance to tight optical filtering as direct detection, while maintaining its advantage in ROSNR. Note that it approaches the performance of duobinary with direct detection after a large number of filter cascades while conventional DPSK with DI FSR=R enjoys an advantage in ROSNR for a P2P system. Interestingly, the duobinary system based on our proposed PI-BD scheme reaches parity with conventional DPSK after only 4 filter cascades, and shows a ~ 0.7 dB better performance after 6 filter cascades. However, DPSK can regain an advantage by employing a DI FSR = 1.2*R. In this case, DPSK shows the best performance up to N ~ 14, at which point the PI-DB scheme achieves parity.

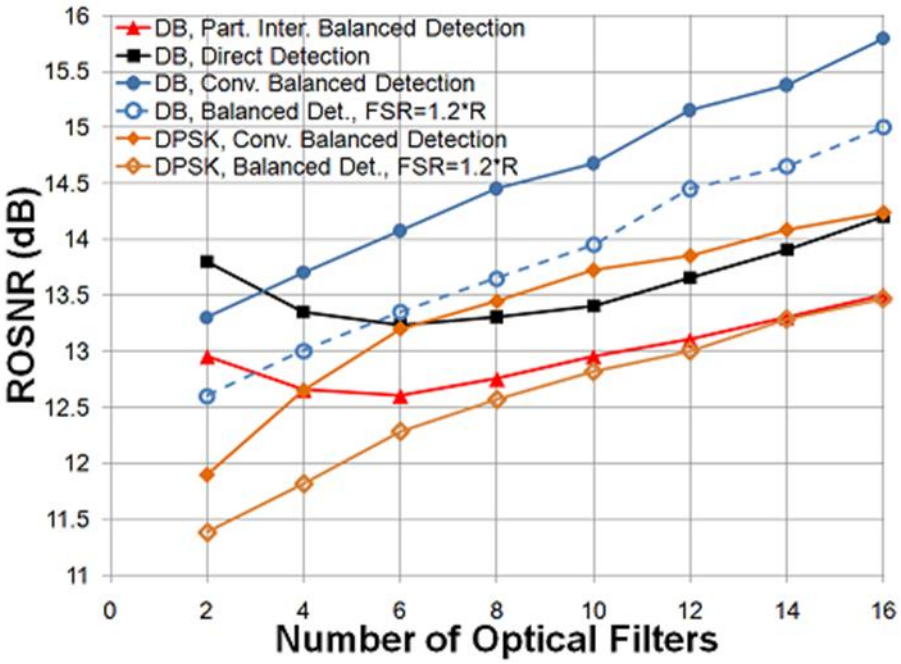

Figure 5.11 Simulated required OSNR versus number of optical filter cascades. Each filter is modeled as a 3rd order super Gaussian with FWHM = 43 GHz.

Figure 5.12 shows the simulation results on the impact of chromatic dispersion for a P2P system design (N = 2). Dispersion penalty is defined in terms of required OSNR to achieve BER = 10^{-3}. As shown in Figure 5.12, the duobinary modulation typically achieves better dispersion tolerance compared with DPSK; this observation remains true even when balanced detection is used to enhance the duobinary receiver sensitivity. Note that the simulated system model includes narrow optical filters (FWHM = 43 GHz), which tend to improve the DPSK dispersion tolerance, bringing it closer to that of duobinary. The PI-BD receiver scheme is particularly interesting for duobinary because it enhances receiver sensitivity, while maintaining a relatively good dispersion tolerance and providing an excellent tolerance to narrow optical filtering in OADM applications.

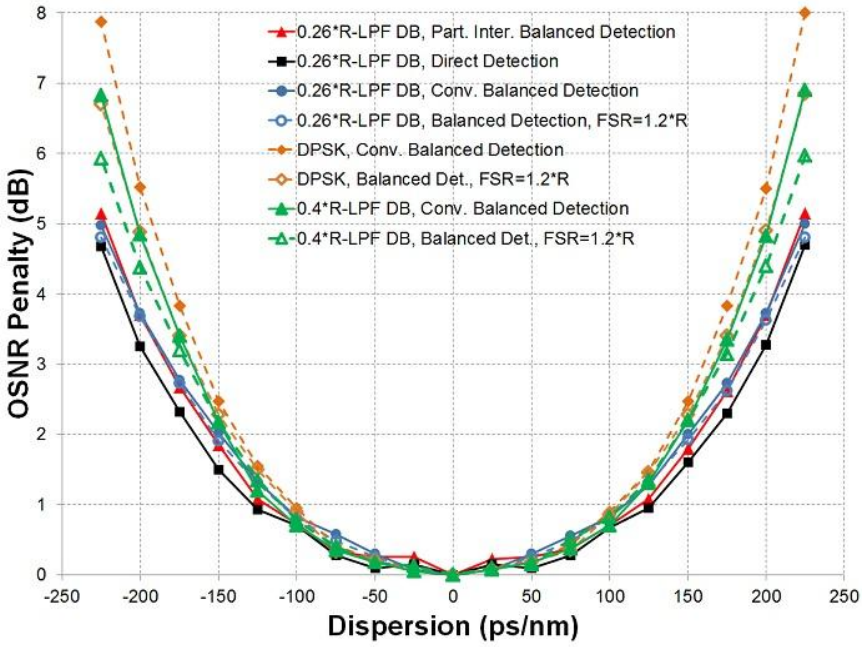

Figure 5.12 Simulated OSNR penalty versus chromatic dispersion for a P2P system.

5.4.2 Nonlinear Regime

The high tolerance to chromatic dispersion and low spectral occupancy make optical duobinary very attractive for deployment of 40 Gb/s modulation format co-existing with 10 Gb/s intensity system[53, 54], while also drawing attentions at long-haul high spectral efficiency systems [55, 56]. However, the impact of fiber nonlinearities on optical duobinary with balanced detection has been fully discussed yet. In Figure 5.13, the impact of nonlinear intra-channel impairments is demonstrated as OSNR penalty versus launched power. Figure 5.13 depicts that PI-BD has the best nonlinear tolerance in the case of 0.26*R-LPF DB. When LPF bandwidth was increased to 40% of bitrate, duobinary with conventional balance detection or with PI-BD comes very close to DPSK.

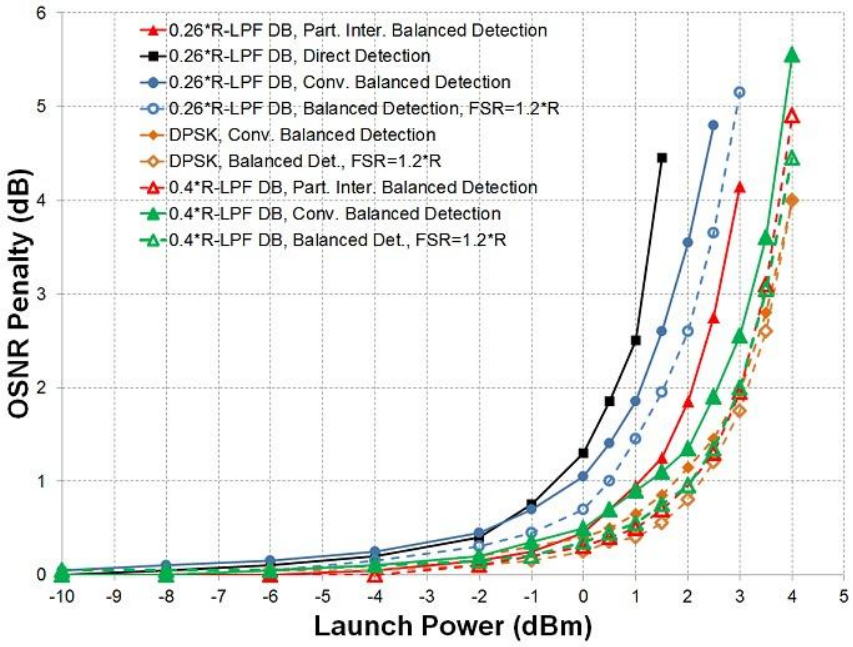

Figure 5.13 Simulated results for the impact of nonlinear phase noise.

5.5 Summary & Conclusions

In this study, we considered balanced detection schemes for LPF generated optical duobinary modulation. Our experimental studies at 10 Gb/s demonstrated a clear benefit in using balanced detection to improve the receiver sensitivity of LPF generated optical duobinary. Balanced detection is especially useful for duobinary modulation when the LPF bandwidth is designed to be wider than the traditional ~ 0.28*R. In this case, duobinary can approach to within ~ 1 dB of DPSK performance while maintaining an advantage in spectral efficiency. Simulation analysis at 42.7 Gb/s confirmed the experimental results, as well as demonstrating a promising balanced detection scheme for mitigating the impact of narrow optical filtering in OADM networks. An extra simulated

discussion for intra-channel nonlinear impairments displays that with balanced detection is more tolerant to intra-channel nonlinear impairments than with direct detection. Moreover, a similar nonlinear tolerance of DPSK can be reached in 40 Gb/s system simulatedly, as deploying 0.4*R-LPF duobinary with balanced detection.

Chapter 6
20 Gb/s DQPSK &
40 Gb/s Polmux-DQPSK

This chapter presents experimental data at 20 Gb/s DQPSK and 40 Gb/s Polmux-DQPSK which discuss the impact of Gordon–Mollenauer nonlinear phase noise induced by intra-channel fiber nonlinearity. We also demonstrate a novel differential quadrature phase-shift keying (DQPSK) receiver based on optical frequency discriminator demodulator with direct detection. The experimental results confirm theory, showing a factor of 2 enhanced tolerance to chromatic dispersion compared with a conventional delay-interferometer-based demodulator with balanced detection. The frequency discriminator direct detection receiver also shows a significant improvement in tolerance to Gordon–Mollenauer nonlinear phase noise.

Section 6.1 briefly illustrates the experimental setup for both DQPSK and Polmux DQPSK systems. In section 6.2, different types of receiver structures are displayed. Section 6.3 and section 6.4 focus on linear and nonlinear regimes, respectively.

6.1 Experimental Setup

6.1.1 DQPSK

Error! Reference source not found.shows a schematic diagram of our 20 Gb/s (10 baud) DQPSK experimental setup for testing linear impairments. The DQPSK modulator

is based on a dual-MZM structure and is specified to have a bandwidth of 8 GHz. The two arms of this DQPSK modulator are driven by the two 10 Gb/s complementary NRZ electrical data sequences of length $2^{15} - 1$ from a pulse pattern generator (PPG). A 26-bit delay inserted between two data streams for decorrelation. The generated DQPSK signal of modulator is fed into a variable optical attenuator (VOA1), which controls the optical power launched into conventional single-mode fiber (SMF-28) of various lengths. The launched power into the fibers is kept at a relatively low value of -3 dBm to suppress nonlinear effects for testing dispersion penalty. The second attenuator (VOA2) is set to control the input power of EDFA that is followed by either an optical frequency discriminator filter or a DI demodulator.

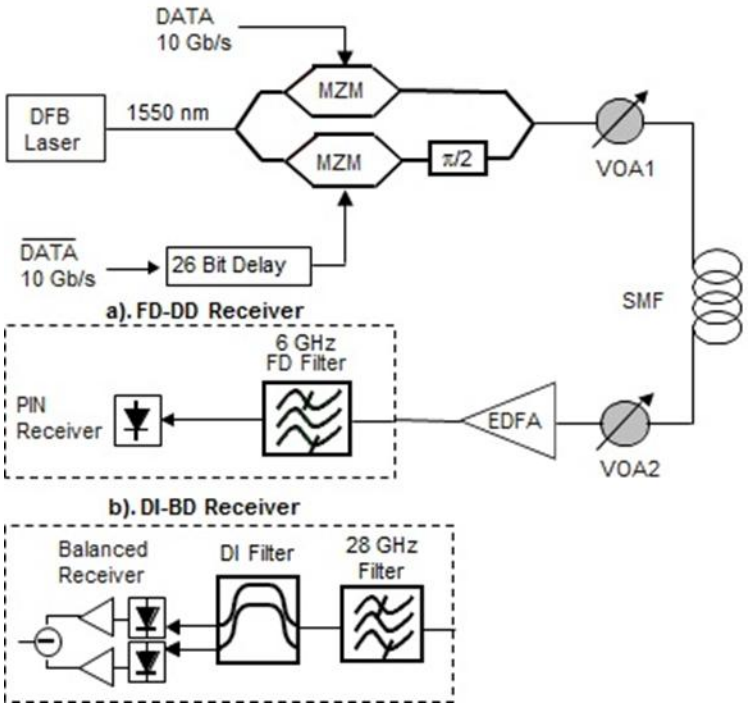

Figure 6.1 Experimental setup for testing 20 Gb/s DQPSK

As can be seen in **Error! Reference source not found.** (b), Experimental setup for esting 20 Gb/s DQPSK the frequency discriminator demodulator employs an optical spectrum analyzer (OSA) operating in a filter mode as a required narrow optical band-pass filter (BPF) which bandwidth is set by the OSA resolution. At an OSA resolution of 0.04 nm, we obtain an approximately Gaussian-shaped optical filter with ~6 GHz bandwidth. Following the frequency discriminator, it is a standard 10 Gb/s OOK receiver, including a p-i-n photodetector, integrated trans-impedance amplifier (TIA), and limiting amplifier (LA), specified to have an electrical bandwidth of 9 GHz. The received optical signal is then converted into electrical signal that is fed into an error detector (ED), programmed for the proper data pattern after demodulation. Clock recovery (CR) is achieved by tapping a portion of the signal at output of discriminator filter demodulator into a commercial instrumental OOK receiver with CR circuitry.

For a reference, we measure the system performance of a conventional DQPSK receiver consisting of a DI and a balanced detector as shown in **Error! Reference source not ound.** (b). The optical filter with FWHM of 28GHz is required for suppressing excess ASE noise as the periodic transfer function of Dis. We also test two DIs with free spectral range (FSR) of 10 and 12 GHz for comparison. The balanced receiver is the same as what we used at previous duobinary experiments in chapter 5. Clock recovery (CR) is achieved by tapping a portion of the light at output of 28 GHz optical filter into a separate DI demodulator, and detecting the constructive port output using the instrumental OOK receiver with CR circuitry.

6.1.2 Polmux DQPSK

Figure 6.2 displays the experimental setup for testing 40 Gb/s Pol-Mux DQPSK modulation format with two different demodulators, frequency discriminator with direct detection (DD) and DI with balanced detection (BD). At transmitter, I and Q, two 10 Gb/s complementary NRZ electrical data sequences of length $2^{15} - 1$ from a pulse pattern generator (PPG) are the drive voltage of DQPSK modulator. Following the DQPSK modulator, a polarization beam splitter (PBS) is deployed to create two orthogonal polarization optical carrier waves. The delay between two orthogonal optical paths is controlled by variable delay tuner. Polarization Switcher is set up in another branch to help modify Polarization controller in the receiver end. Thus, the optical carriers of each optical polarization contain 20 Gb/s (10Gbaud) DQPSK data, then being combined by a Polarization Beam Combiner (PBC) to produce a 2x20Gb/s Pol-Mux DQPSK signal.

The generated Polmux-DQPSK signal is fed into a variable optical attenuator (VOA1), which controls the optical power into the transmission link for measuring the impact of Gordon-Mollenauer nonlinear effect. This transmission link will be explained in section 6.1.3. For the measurements of linear impairments, the optical power launched into conventional single-mode fiber (SMF-28) of various lengths is kept at a relatively low value of -3dBm to suppress nonlinear effects for testing dispersion penalty, which is similar to 20Gb/s DQPSK experimental setup.

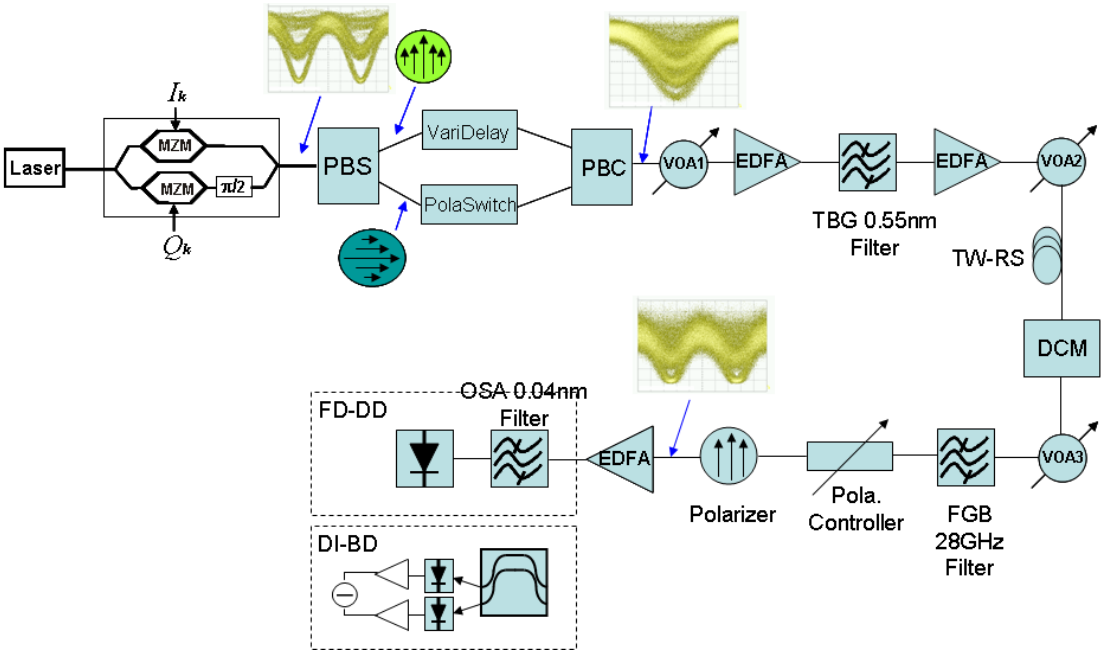

Figure 6.2 Experimental Setup of 40 Gb/s Polmux DQPSK

To detect the information carried by the light of two polarizations, we utilized a polarization controller followed by a polarizer. The dynamic polarization controller is helpful to stabilize the polarization of carrier waves due to the time-variable property of polarization status. The optical carried of linear polarization is fed into a polarizer that filters out undesired polarization component. In a practical implementation, a polarization beam splitter would be employed instead of a polarizer in order to receive the signals in both polarizations simultaneously. Then each signal is received by a separate DQPSK receiver to extract the transmitted information. Similar to the previous experiment of DQPSK, two types of demodulator, the conventional receiver based on delay interferometer and the proposed receiver based on frequency discriminator are compared in this experiment.

6.1.3 Transmission setup for Gordon-Mollenauer nonlinear effect

As depicted in section 3.2, the Gordon-Mollenauer nonlinear phase noise generated during long-haul transmission links as the signal beats with ASE noise via fiber Kerr nonlinearity is an important impairment for phase modulation formats. To produce a sufficiently strong nonlinear phase shift with a shorter fiber, we replace standard single mode fiber (SMF-28) in the experimental setup of Figure 6.3 with a 50 km TW-RS fiber that has a smaller effective area of -40mm2. A smaller core effective area can increase nonlinear coefficient.

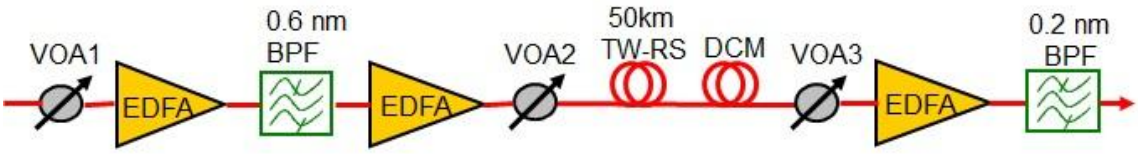

Figure 6.3 Transmission setup for Gordon-Mollenauer nonlinear effect.

The transmission setup is shown schematically in Fig. 6. We utilized VOA1 and VOA2 to control OSNR and to modify the launched power the fiber span, separately. Launch OSNR was kept fixed at relatively low value of 18 dB to enhance as the signal beats with ASE noise. The dispersion of TW-RS fibers is compensated by a DCM. Meanwhile, we set VOA3 to control received OSNR at 15dB. Such a fiber span is able to provide DQPSK an average nonlinear phase shift of 0.5 rad ($\gamma = 1.9W^{-2}km^{-1}$) at the output of the fiber span according to according to theory.

6.2 Receiver Structures

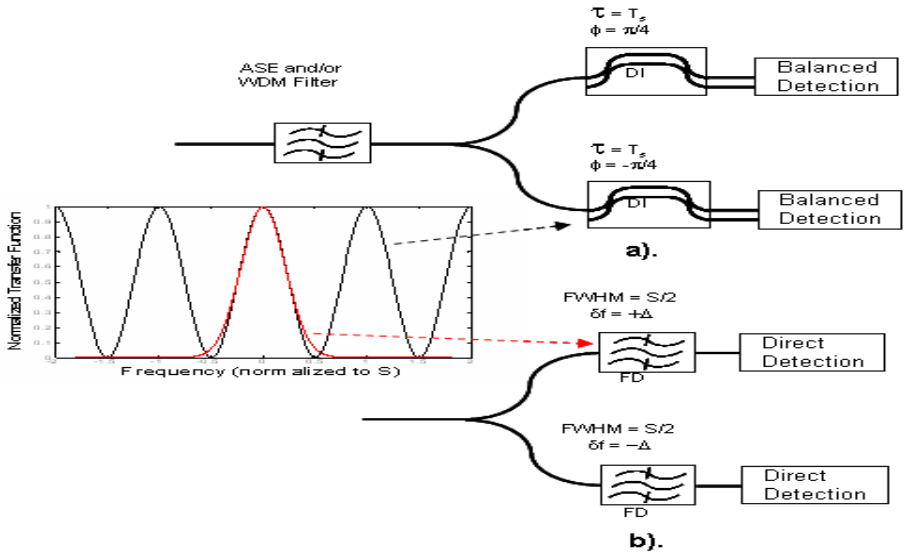

Figure 6.4 Schematic diagram for DQPSK receiver based on: (a) DI demodulators and balanced detection and (b) FD filters and direct detection.

DQPSK demodulator is a key component to translate the optical phase modulation into intensity modulation for square-law detection at the receiver. As can be seen in Figure 6.4 (a), a typical method of DQPSK demodulator is using a Mach-Zehnder delay interferometer followed by a balanced detector to demodulate each quadrature. The differential delay of each DI is a symbol period T_s with the baud rate S = 1/T_s. Each DI is phase shifted by +π/4 or –π/4 to decode the in-phase or quadrature phase. The opposite phases of two DIs are equivalent to opposite frequency detuning of δf = $\pm S/8$ relative to carrier frequency. Some disadvantages of the conventional DQPSK receiver including a high complexity, relatively poor tolerance to chromatic dispersion (CD), severe sensitivity to frequency offsets [57-59], and vulnerability to nonlinear phase noise induced by the intra-channel fiber nonlinearity [28].

Note that optical phase shifts between each quadrature in time are equivalent to frequency variations. Thus, it is possible to replace DI with an optical frequency discriminator filter to serve as a demodulator. In Figure 6.4 (b), our proposed DQPSK receiver of a lower complexity is schematically illustrated. The DIs are replaced by Gaussian-shaped band-pass optical frequency discriminator filters with full-width at half-maximum (FWHM) ~ S/2, and opposite frequency detuning of $\pm\Delta$. According to simulation analysis, the optimized frequency shift was found to be Δ = ~0.173S. Following the frequency discriminator, it is simple direct detection with single photodetector. With such a design, no additional optical filtering is necessary since the narrow band-pass frequency discriminator filter provides excellent isolation from adjacent WDM channels and/or amplified spontaneous emission (ASE) noise suppression. In the following sections, we report the experimental demonstration of the proposed DQPSK demodulator, and compare its performance with the conventional DI-based approach.

6.3 Tolerance to Linear Impairments

In this section, the tolerance to linear impairments is studied through experimental results of back-to-back (B2B) receiver sensitivity and dispersion penalty, at 20 Gb/s DQPSK and 40 Gb/s Polmux-DQPSK. In addition, we compare frequency discriminator demodulator followed by direct detection (FD-DD) with DI of FSR = 12 GHz and 10 GHz followed by balanced detection (DI-BD).

6.3.1 20Gb/s DQPSK

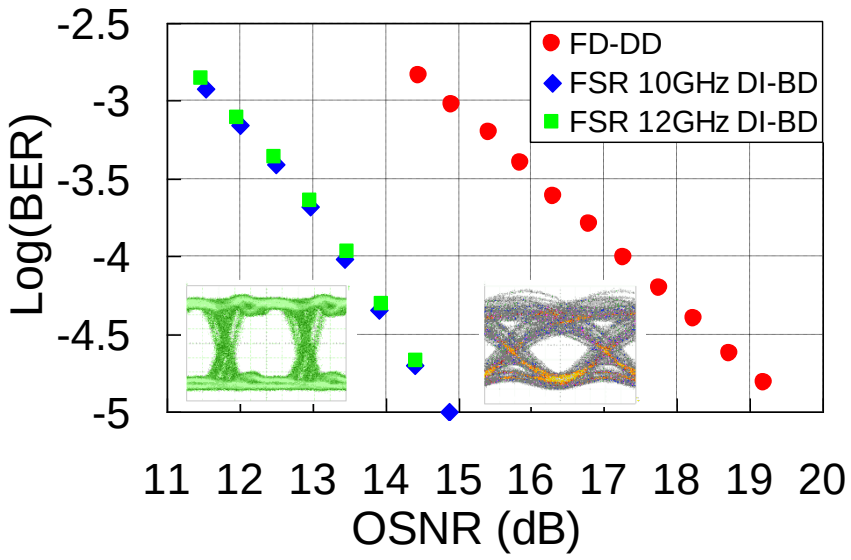

Figure 6.5 Back-to-back measured BER versus OSNR for FD-DD and DI-BD (FSR 10 and 12 GHz).

Figure 6.5 displays B2B bit error rate (BER) as a function of OSNR measured at the output of EDFA preamplifier in Figure 6.2**Error! Reference source not found.**. The BER is obtained by averaging the measured OSNRs of I and Q. For DI-BD, we tested two DIs, one DI with FSR exactly equal to baud rate (R) and another one with FSR equal to 1.2*baud rate (12GHz). It is interesting to make a comparison between DI with FSR equal to R and another DI with wider FSR due to the potential enhancement of chromatic dispersion in DPSK using DI demodulator with differential delay less than a symbol period [52]. As can be seen in Figure 6.5 the required OSNR of both DI-BD receivers is measured to be ~11.7 dB at BER of 10^{-3}. The DI of wider FSR suffers no penalty in our system because the DQPSK modulator has a relatively narrow ~8 GHz bandwidth, which means a wider FSR DI can compensate the impact of narrow optical filtering.

At DI-DD receiver, the tributaries of I and Q are able to be switched for demodulation through detuning the discriminator filter center by $\sim \pm 1.7\text{GHz}$ away from Laser frequency. For BER = 10^{-3}, the required OSNR of FD-DD receiver is ~3.2 dB more than DI-BD receiver due to the sensitivity advantage of balanced detection over direct detection. At lower BER, the data show a greater difference, approaching 4 dB at BER of 10^{-4}.This can be also realized through the noise-free eye diagrams displayed in Figure 6.6. The square-like eye of DI-BD measured after balanced receiver shows a better eye opening over the duobinary-like eye of FD-DD measured directly after frequency discriminator filter. The difference between two eyes may explain the relatively poor OSNR sensitivity of FD-DD for lower BER. But, a duobinary-like eye might potentially contribute a better tolerance to chromatic dispersion.

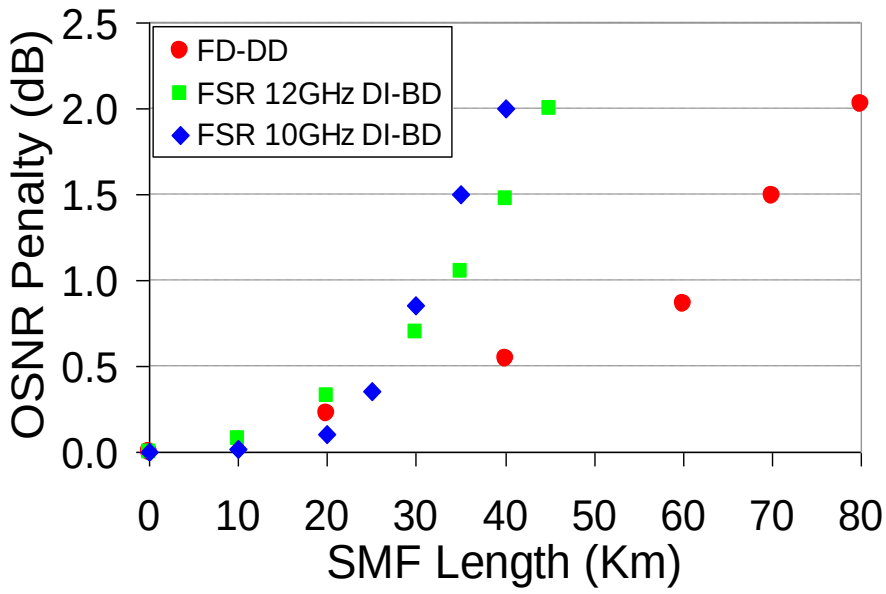

Figure 6.6 Experiment Results of Dispersion Penalty

Another comparison of tolerances to chromatic dispersion is presented in Figure 6.6, where the measured OSNR penalty as a function of SMF (D = ~17 ps/(nm*km)) transmission distance is illustrated. OSNR penalty is defined as relative variation of B2B performance at BER equal to 10^{-3}. FD-DD demonstrates an advantage of a factor of 2 in dispersion tolerance in comparison to DI-BD receiver. This experimental data confirm our previous theoretical predictions [60]. Note that FD-DD receiver with DI of wider FSR enables 10Gbaud DQPSK to transmit over 44 km without dispersion compensation, while FD-DD receiver admits an impressive 80 km SMF transmission distance. The ultra-narrow frequency discriminator filter shows a more effective suppression to deleterious high-frequency signal pulse, even compared with DI filter with an optimized FSR. It is also interesting to realize the impact of FSR on the dispersion tolerance of DI-BD receiver. The 20% wider FSR DI shows a 12.5% improvement in CD tolerance at 2 dB OSNR penalty, roughly in line with the theoretical predictions in [52] for DPSK.

6.4 Analysis of Nonlinear Regime

In this section we discuss the impact of nonlinear phase noise generated by intra-channel nonlinear effect also known as Gordon–Mollenauer effect on DQPSK and Polmux-DQPSK systems.

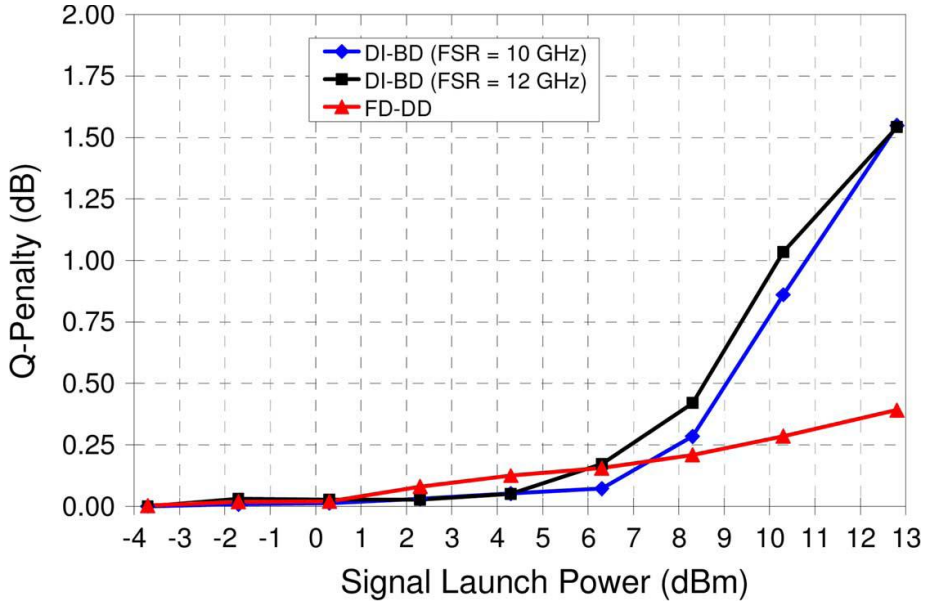

Figure 6.7 Measured *Q*-penalty versus signal launch power for DQPSK.

Due to high nonlinear sensitivity of high spectral efficiency modulation formats, it is important to discuss the tolerance to nonlinear phase noise for different receiver structures. Figure 6.7 shows the nonlinear *Q*-penalty as a function of launch power. Instead of measuring OSNR, we evaluated *Q*-factor while keeping received OSNR fixed at 15dB. *Q*-factor is obtained from the measured BER for each value of launch power into the fiber span. At low launch powers of dBm, both FD-DD and DI-BD receivers show a negligible nonlinear *Q*-penalty. However, as we continue to increase launch power, the *Q*-values drop due to nonlinear effect, and we observe a measurable *Q*-penalty. The conventional DI-BD receiver obtains a 1 dB Q nonlinear penalty at a launch power of 11 dBm in approximate agreement with theory. We define the nonlinear threshold as the launch power corresponding to a 0.5 dB Q penalty. Thus, DQPSK with conventional DI-BD receiver reaches its nonlinear threshold at 9 dBm for our single-span system.

Using a wider FSR DI demodulator provides no noticeable benefit in nonlinear tolerance in our experiment. However, the FD-DD receiver shows 4 dB greater nonlinear threshold, a very significant enhancement in nonlinear tolerance compared to DI-BD receiver. Thus, while direct detection may hurt the FD-DD scheme in OSNR sensitivity compared with DI-BD in a linear regime, it provides a significant benefit for nonlinear transmission.

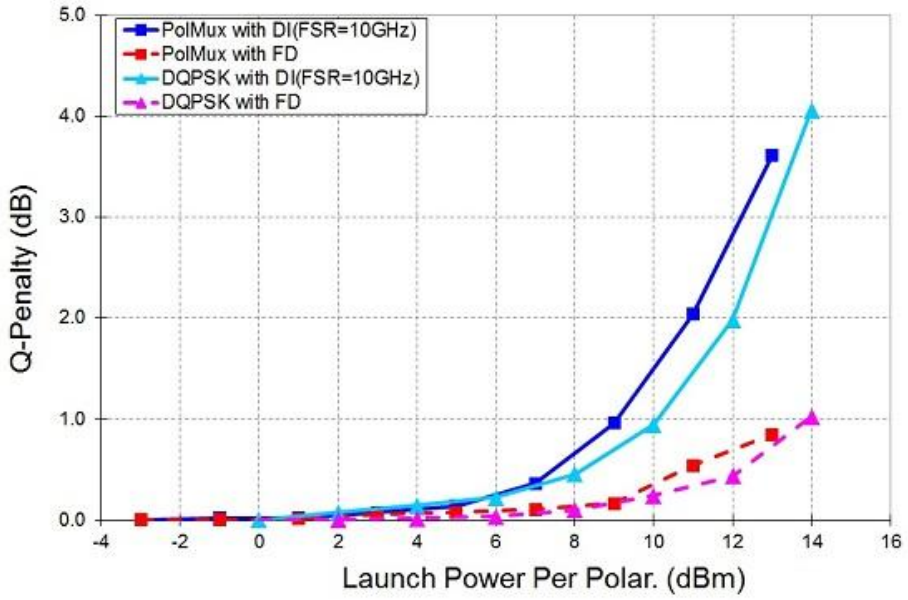

Figure 6.8 Measured *Q*-penalty versus signal launch power for Polmux-DQPSK.

It is also interesting to know whether FD-DD still maintains the advantage of nonlinear tolerance over conventional BD-DI at 40 Gb/s Polmux-DQPSK systems. As can be seen in Figure 6.8 Measured *Q-penalty* versus signal launch power for Polmux-DQPSK., both receivers have similar tolerance to the intra-channel nonlinear effect, alongside demonstrating very close Q-penalty as a function of launched power into fibers. Thus,

FD-DD still keeps the same benefits of nonlinear tolerance, displaying 4 dB greater nonlinear threshold in Polmux-DQPSK transmission systems.

6.5 Summary & Conclusions

A novel low complexity DQPSK receiver based on frequency discriminator filter demodulator is demonstrated experimentally at 10 Gbaud, and compared with conventional balanced detection with delay interferometer. The FD-DD received shows a factor of 2x enhanced tolerance to chromatic dispersion, while demonstrating ~4 dB higher nonlinear threshold to Gordon–Mollenauer effect for both DQPSK and Polmux-DQPSK systems, compared with conventional DI-BD receiver.

Even though FD-DD receiver has a relatively poor OSNR sensitivity, ~ 3 dB worse compared with DI-BD receiver at BER = 10^{-3}, the lower complexity FD-DD receiver architecture, taken together with its good dispersion and fiber nonlinearity tolerance, may offer an interesting alternative for future 100G metro systems provided OSNR sensitivity is not the major design constraint.

Chapter 7
100 G Polmux-QPSK Simulation

Increasing spectral efficiency and bit rate per channel are major drivers in modern fiber-optic communications, with recent research efforts focused on so-called 100G systems to enable efficient transport of 100 Gb/s Ethernet traffic [13, 61]. The dual polarization quadrature phase shift keying (DP-QPSK) modulation format in combination with coherent intra-dyne detection has received much attention recently as a prime candidate for 100G systems. With typical baud rates of ~ 25-28 Gbaud, the DP-QPSK format has sufficient spectral efficiency to fit on the standard 50 GHz ITU grid. QPSK optoelectronic modulator technology is well developed, and recent advances in digital coherent receivers enable polarization de-multiplexing in the electrical domain, with efficient equalization of linear impairments such as dispersion and PMD. Moreover, the coherent detection of QPSK provides an excellent OSNR sensitivity, which is important for long-haul transmission systems. However, the tolerance to nonlinear transmission effects is a major concern for coherent QPSK systems [62, 63]. Cross phase modulation (XPM) from neighboring WDM channels results in deleterious nonlinear phase noise and nonlinear polarization scattering or cross polarization modulation (XPOLM). The XPOLM is particularly troublesome in systems employing polarization multiplexing [64]. Very promising recent research has shown that symbol-interleaving of RZ pulses can significantly reduce the impact of XPOLM on coherent DP-QPSK systems [65].

In this chapter, we employ rigorous Monte-Carlo computer simulations to study the impact of pulse shape on the nonlinear benefit of symbol-interleaving. Our numerical studies reveal several interesting engineering tradeoffs between spectral efficiency and nonlinear tolerance. In particular, while the RZ format is preferred over NRZ for nonlinear tolerance, there is little benefit in using the narrowest RZ pulse shapes, e.g. the 67% duty cycle RZ pulse performs just as well as 50% duty cycle RZ. In contrast to previous research [65], we also show that even NRZ systems can gain a significant improvement in nonlinear tolerance from symbol interleaving. The optical line system dispersion map plays an important role on the impact of pulse shape in the nonlinear regime.

7.1 Simulation Model

In fiber-optic transmission systems, the choice of pulse shape is typically limited by the hardware to two alternatives: non-return-to-zero (NRZ) or return-to-zero (RZ). The NRZ-QPSK modulator is shown schematically in Figure 7.1 a). RZ pulse carving is realized with an additional Mach-Zehnder modulator (MZM). Several flavors of RZ are possible using the pulse carver MZM, depending on driver signal voltage amplitude and MZM bias conditions. In the following, we consider 50% duty cycle RZ (RZ50), and 67% duty cycle RZ (RZ67), as shown schematically in Figure 7.1 b). and c)., respectively. The corresponding pulse shapes are visualized in Figure 7.1 using eye diagrams.

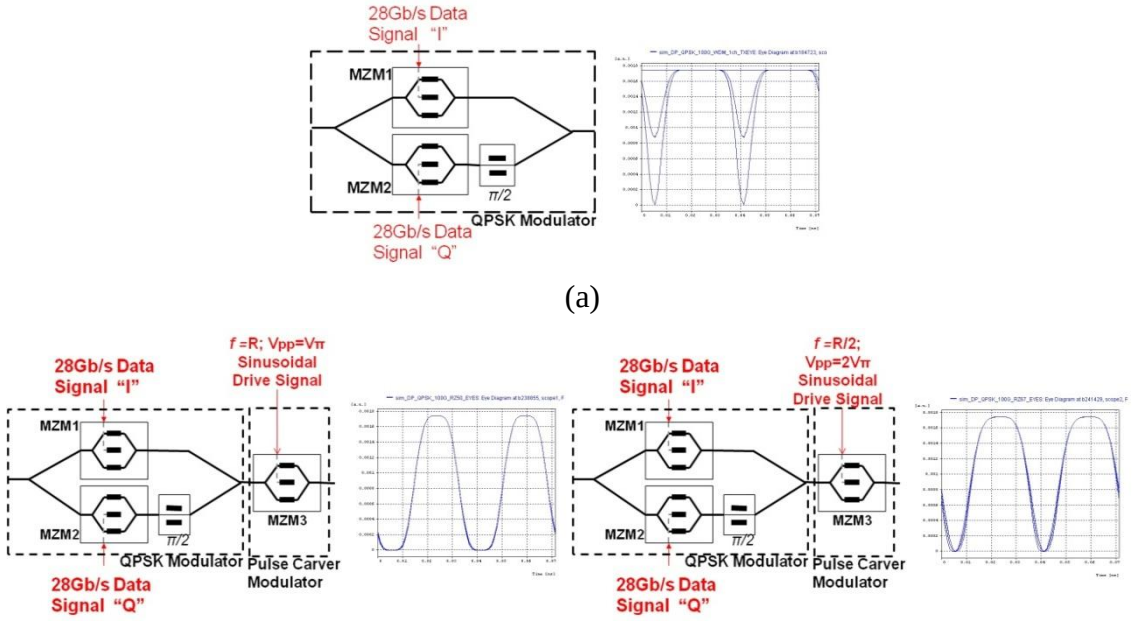

Figure 7.1 Modulator structures and simulated pulse waveforms for a) NRZ, b) 50% duty cycle RZ, and c) 67% duty cycle RZ.

Note that in linear systems, the receiver performance is in principle independent of pulse shape, as long as a matched filter is used at the receiver to optimize the signal-to-noise-ratio (SNR) at the decision gate. In practice, the RZ pulse shape is preferred over NRZ even in linear transmission because RZ pulses are inherently more tolerant to inter-symbol interference (ISI) [66]. In nonlinear transmission, the choice of pulse shape is even more important. In particular for DP-QPSK transmission, the RZ pulse shape in combination with symbol-interleaving of X and Y polarization tributaries was shown to suppress nonlinear XPOLM [64, 65]. Due to symbol-interleaving, the state-of-polarization (SOP) alternates between X and Y polarizations for successive symbols, leading to a cancelation effect of XPOLM as adjacent WDM channels walk through each

other during propagation. Intuitively, one may assume, as was done in [65], that only an RZ pulse shape can benefit from symbol-interleaving. However, we show below that NRZ can also benefit, albeit substantially less so than RZ. It is also interesting to consider the impact of RZ pulse duty cycle on nonlinear performance. While narrower RZ pulses lead to a sharper contrast between the X and Y polarizations in symbol-interleaved transmission, there is a negative trade-off in spectral efficiency; the simulated power spectra for 28 Gbaud NRZ-QPSK, RZ50-QPSK, and RZ67-QPSK are shown in Figure 7.2.

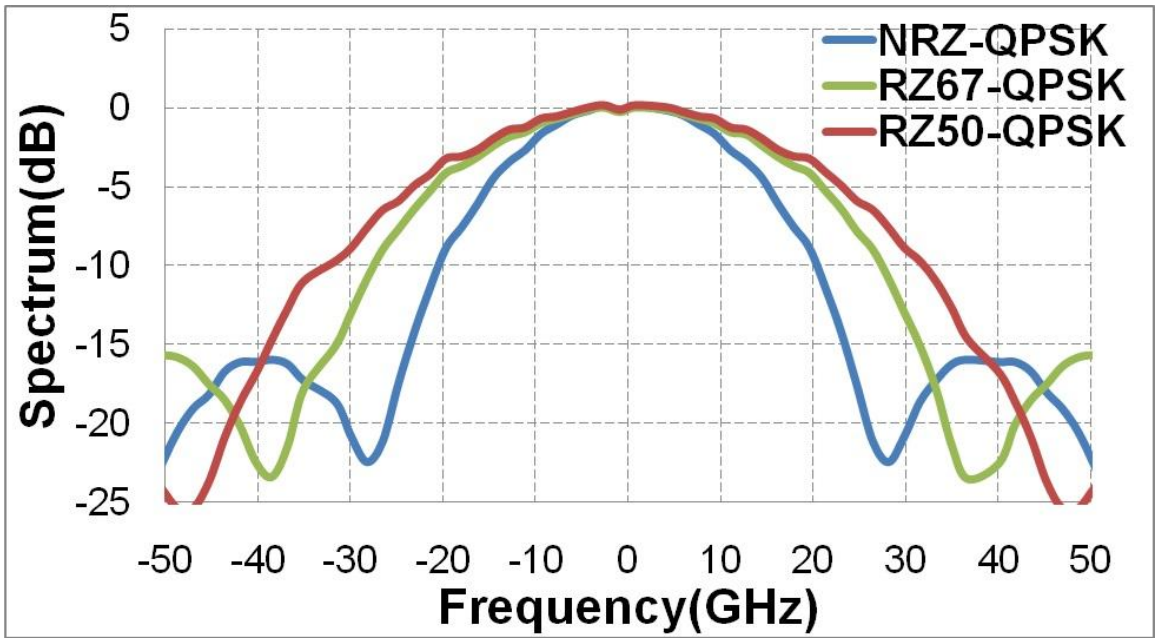

Figure 7.2: Simulated optical power spectra at the output of modulator.

The IQ modulators of Figure 7.1 are driven by independent PRBS data patterns of length 2^{16} at a symbol rate of 28 Gbaud. The modulator electro-optic frequency response is modeled by a 5-pole Bessel low-pass filter (LPF) with bandwidth equal to baud rate

applied to the drive signals. A total of 9 WDM channels are transmitted with a channel spacing of 50 GHz, including random timing shifts between the data patterns of different channels for de-correlation. The WDM multiplexing and de-multiplexing filters are modeled as 2^{nd} order super Gaussian optical filters with a 40 GHz bandwidth.

To assess the nonlinear tolerance of the various modulation formats described above, we simulate nonlinear propagation over 1000 km (10 spans x 100 km) of standard single mode fiber (SSMF) with dispersion D = 16.5 ps/nm/km and nonlinear coefficient = 1.3 $W^{-1}km^{-1}$. Amplified spontaneous emission (ASE) noise is loaded at the output of the transmission line to set the optical signal to noise ratio (OSNR) at the receiver. The center WDM channel is selected by the WDM de-multiplexer and passed to the digital coherent receiver. Receiver front-end electrical bandwidth is 70% of baud rate, modeled by 5-pole Bessel LPF. The demodulated I/Q signals are sampled once per symbol at symbol center, and the carrier phase is estimated using the gliding window feed-forward technique proposed by Noe [67] with a block size of 11 samples. Note both transmitter and local-oscillator lasers each have a linewidth of 1 MHz The bit error rate (BER) is calculated by error counting to find the required OSNR for BER = 10^{-3}.

7.2 Nonlinear Transmission over Distributed Map

Initial “brown field” deployments of 100G technology would have to work on optical line systems designed for legacy 10G (typically OOK) systems. Such systems are based on *distributed dispersion maps*, where dispersion compensating fiber (DCF) is placed at each amplifier node to carefully manage the accumulated dispersion. In this section, we

compare the performance of 100G DP-QPSK with various pulse shapes on distributed dispersion maps. A typical distributed dispersion map is shown in **Error! Reference ource not found.**, where the DCF is chosen to slightly under-compensate the transmission fiber dispersion by +50 ps/nm at each span. This residual dispersion-per-span (RDPS) allows for some walk-off of the WDM channels between each span, which helps to reduce the impact of interchannel nonlinear effects such as XPM in legacy 10G systems; this walk-off due to RDPS also helps to reduce XPOLM for DP-DPSK systems.

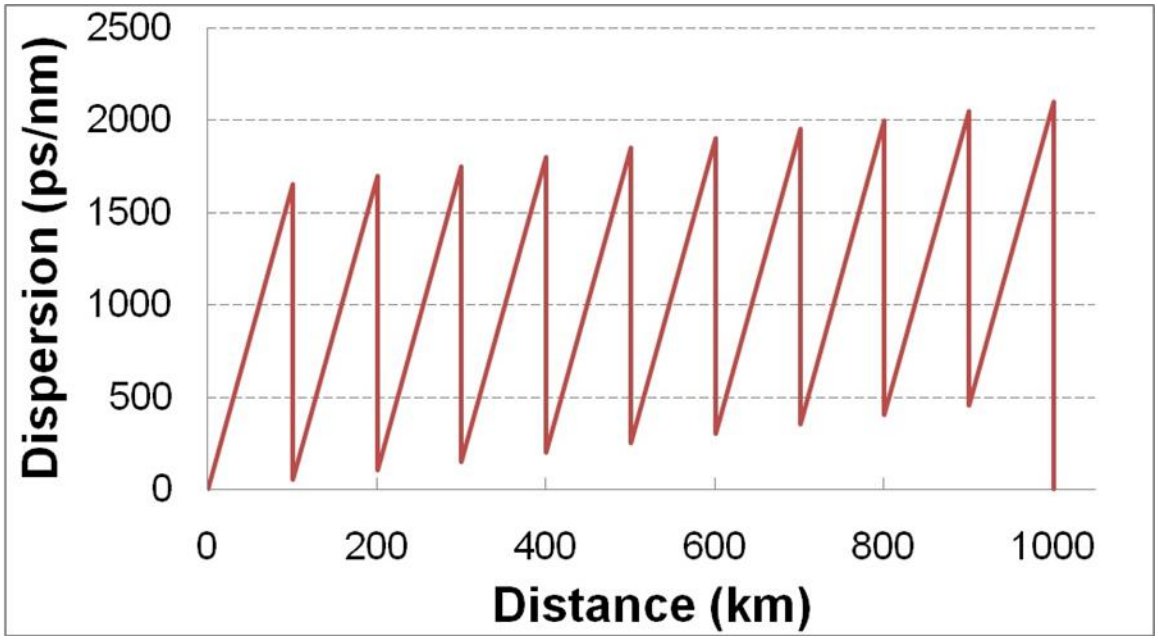

Figure 7.3 Distributed DCF based dispersion map with RDPS = 50 ps/nm.

Error! Reference source not found. shows the simulated nonlinear OSNR penalty at ER=10^{-3} as a function of launched power per channel for the dispersion map of Figure 7.1. Note a typical rule of thumb used by system designers is to raise the launch power up to the point where nonlinear penalty is ~ 1dB. Going far beyond the 1 dB penalty point is

not beneficial because the nonlinear OSNR penalty starts to scale faster than the increase in received OSNR. As can be seen in **Error! Reference source not found.**, there is no ignificant benefit in using RZ modulation for the symbol-aligned formats; they all reach the 1 dB nonlinear penalty point at a launch power of about ~ -1 dBm. Symbol-interleaving dramatically improves the nonlinear tolerance by roughly 2 dB, raising the allowable launch power to ~ +1 dBm for RZ formats; in this case the RZ modulation outperforms NRZ by about ~ 1 dB Note however that the narrower pulse RZ50 format shows about the same performance as RZ67.

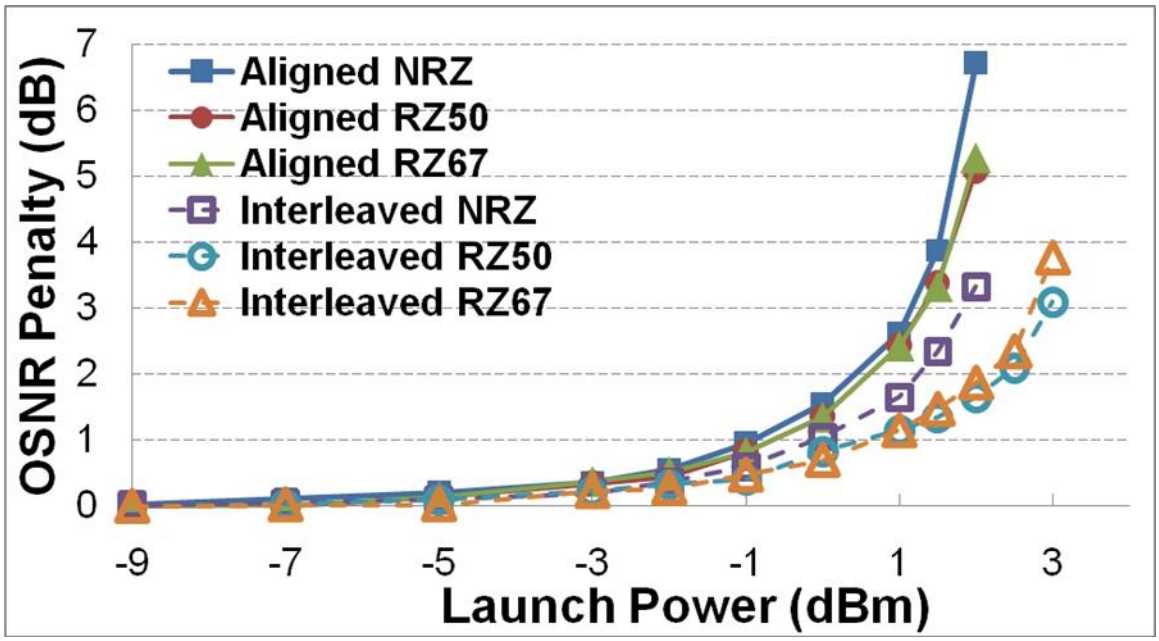

Figure 7.4 Simulation of nonlinear penalty on distributed dispersion map

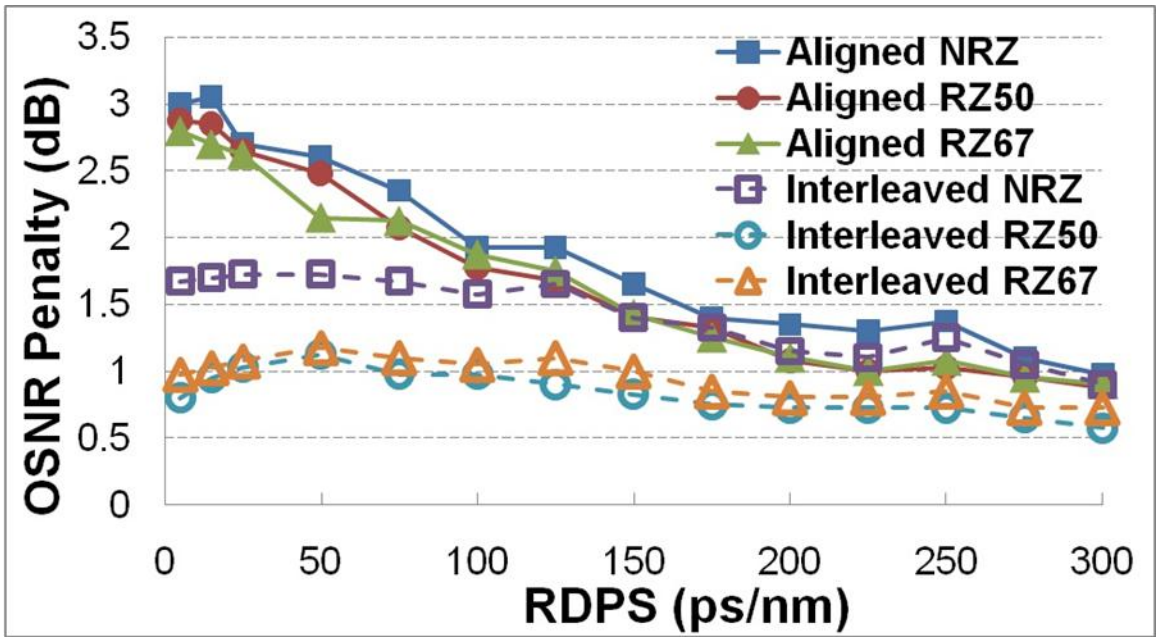

Figure 7.5 Distributed DCF based dispersion map with RDPS = 50 ps/nm.

The impact of RDPS is studied in Figure 7.5. As RDPS is varied in the simulation, the total residual dispersion is always compensated back to zero at the end of the transmission line, and launch power is kept fixed at +1dBm. As expected, the nonlinear penalty is reduced by increasing RDPS due to greater walk-off between WDM channels. Interestingly, the symbol-aligned formats gain the most from increasing RDPS. For symbol-interleaving, the performance improvement is small because while increasing RDPS increases walk-off, it also leads to a greater accumulation of dispersion along the transmission path. This effect broadens the pulses, thus partially offsetting the benefit of symbol-interleaving. The improvement in nonlinear tolerance with increasing RDPS saturates at about +300 ps/nm, at which point the symbol-aligned formats perform only slightly worse than symbol-interleaved.

7.3 Nonlinear Transmission over Lumped Map

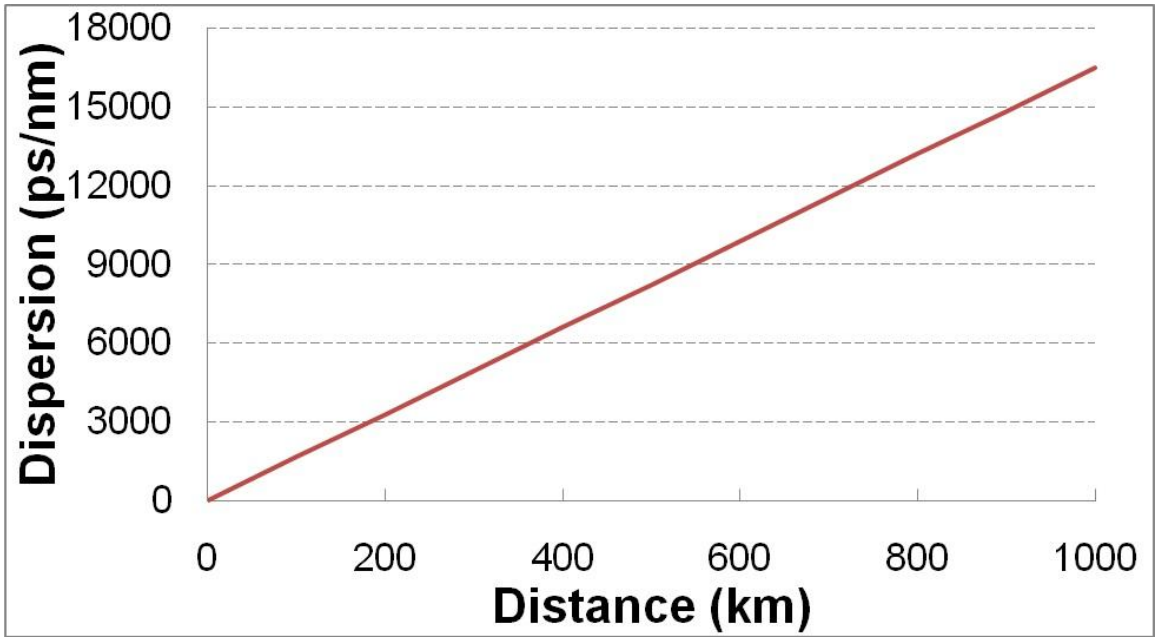

Figure 7.6: Lumped dispersion map with DCF completely removed from system.

The digital coherent receiver is expected to greatly simplify future optical line systems by fully compensating the transmission fiber dispersion in the DSP [68]. This technological advance will free system designers to engineer more cost effective and flexible optical line systems without the need for DCF. Moreover, recent research has shown that removing DCF from the transmission path can also improves the nonlinear tolerance of DP-QPSK. In this section, we compare the nonlinear transmission performance of various pulse shapes for DP-QPSK transmission over the *lumped dispersion* map shown in Figure 7.6. In the modeling of lumped dispersion map, the DCF is completely removed from the optical line system, and we use an ideal frequency domain compensation algorithm (equivalent in optical domain to the action of an ideal lumped DCF at the

receiver) to perfectly compensate the total accumulated dispersion in the digital domain of the coherent receiver model before performing the phase estimation.

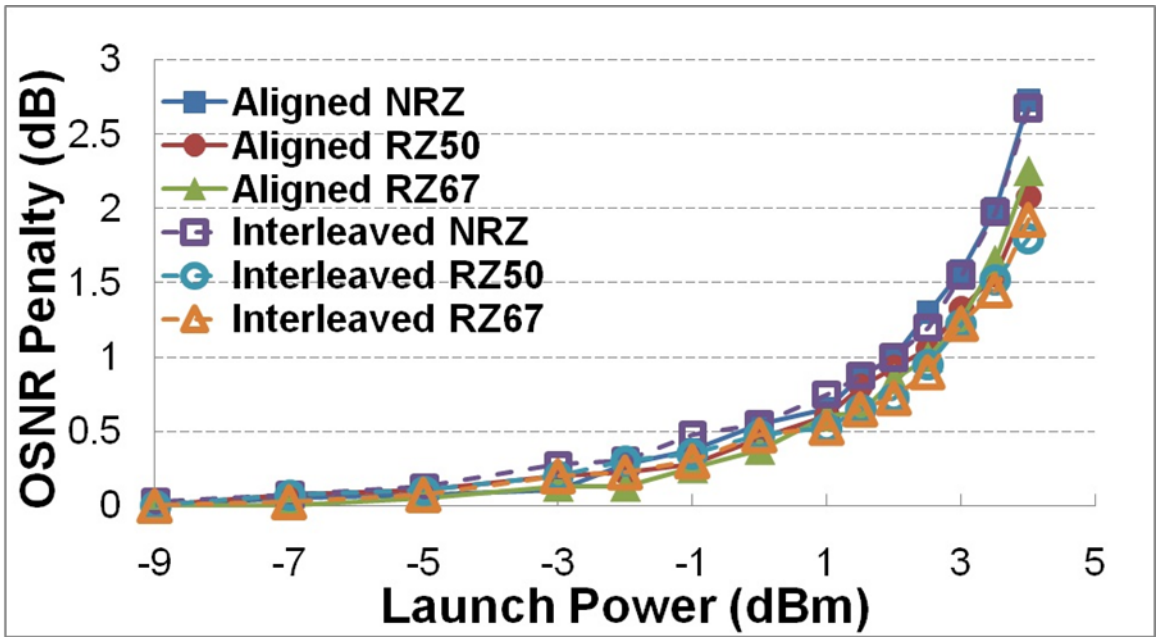

Figure 7.7 Simulation of nonlinear penalty on distributed dispersion map.

Figure 7.7 shows the simulation results on OSNR penalty versus launch power for the lumped dispersion map. In this case, we observe no significant advantage for symbol-interleaving, and no significant advantage for any particular pulse shape. The latter result can be understood by considering that the transmitted signals rapidly lose their original pulse shape as they disperse during propagation without any DCF to restore the pulse shape as in a distributed map. By the same token, the large walk-off between WDM channels (note RDPS is effectively equal to span dispersion) suppresses the inter-channel nonlinear effects. Also, as noted in [65], the strong dispersion spreads the SOP at symbol center over the Poincare sphere, thus averaging out the nonlinear polarization scattering or XPOLM effect. Indeed, the lumped dispersion map provides a better suppression of

nonlinear effects compared with distributed map; the launch power corresponding to 1 dB nonlinear penalty is increased by about ~ 1.5 dB compared with the best symbol-interleaved case on a distributed map.

7.4 Impact of Optical Filtering and Symbol Misalignment

7.4.1 Impact of Optical Filtering

At the high spectral efficiency considered in this study, i.e. 28 Gbaud on 50 GHz channel spacing, the narrow optical filtering in the WDM multiplexer, or optical add-drop multiplexers (OADMs) placed along the transmission path, may have an impact on the nonlinear transmission performance. In this section, we investigate the impact of optical filtering, emulating the effective narrowing of the signal optical bandwidth by simultaneously varying the WDM multiplexer and de-multiplexer optical bandwidths.

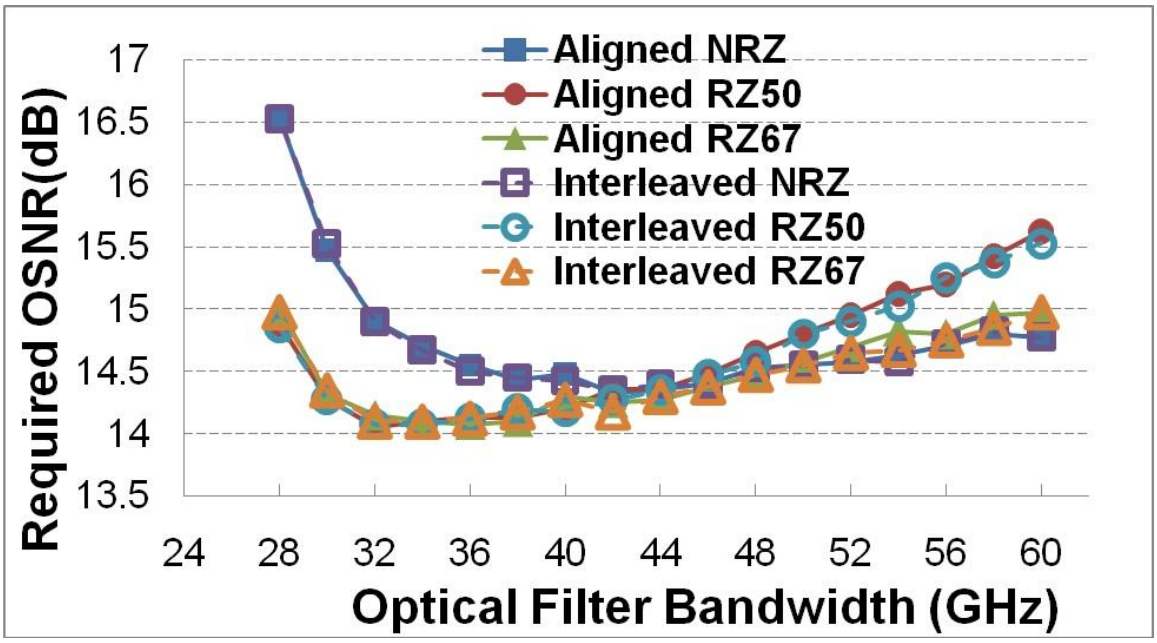

Figure 7.8 Nonlinear penalty as a function of RDPS; launch power is fixed at +1 dBm.

Error! Reference source not found. shows the impact of optical filtering in the linear egime, plotting the required OSNR for BER=10^{-3} as a function of optical filter bandwidth. In a linear system, there is no difference between symbol-aligned or –interleaved formats. In this case, RZ modulation prefers a slightly narrower optical bandwidth compared with NRZ because of WDM linear crosstalk; note the wider spectrum of RZ signal is more susceptible to crosstalk. **Error! Reference source not found.** also shows that the RZ67 format starts to outperform RZ50 for optical bandwidths wider than ~ 45 GHz due to a more compact spectrum.

Figure 7.9 shows a similar simulation as in **Error! Reference source not found.** but in a onlinear regime, corresponding to a distributed dispersion map with launch power of +1 dBm. In the nonlinear regime, an additional interesting trade-off becomes visible: the

optimum optical bandwidths shift perceptibly toward larger values for the symbol-interleaved case. A wider optical bandwidth is preferred for symbol-interleaved transmission to preserve the signal integrity of the pulse shape, and hence the effectiveness of symbol-interleaving.

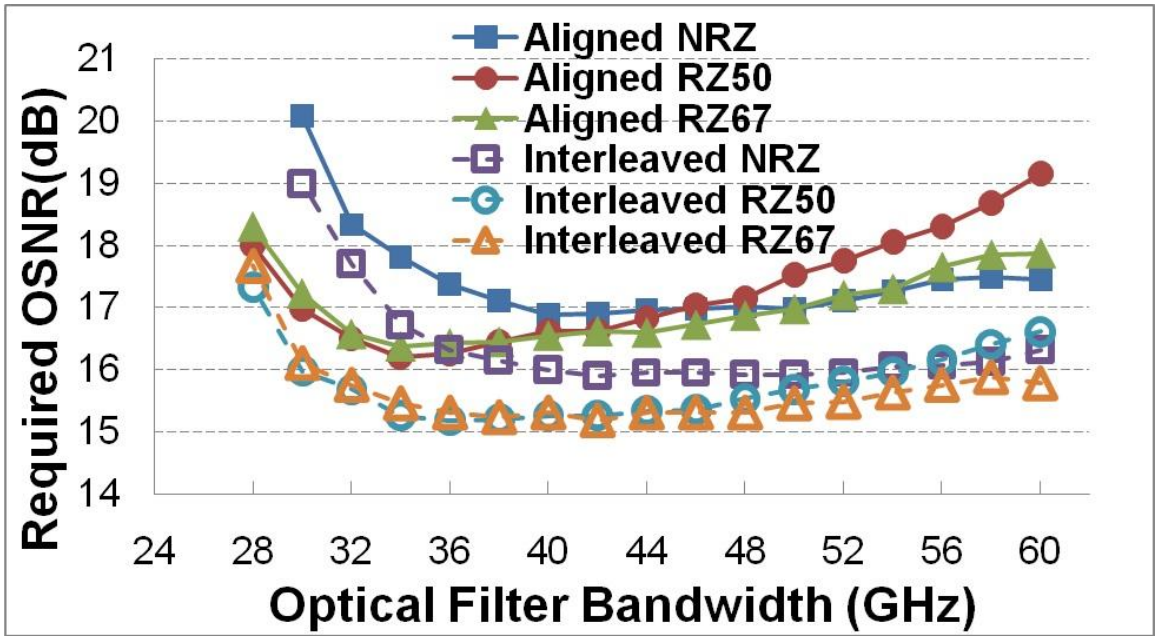

Figure 7.9: Simulation of nonlinear penalty on lumped dispersion map.

7.4.2 Impact of Symbol Misalignment

The good nonlinear tolerance of symbol-interleaved formats depends not only on the signal integrity of the pulse shape but also on maintaining the half-symbol delay between X/Y polarization tributaries during transmission. The accuracy of symbol-interleaving can be compromised by manufacturing tolerances in the transmitter, as well as polarization mode dispersion (PMD) in the transmission line. While a detailed simulation analysis on the impact of PMD is beyond the scope of this study, we can gain some appreciation on the required symbol-interleaving accuracy by considering how the

nonlinear penalty changes as a function of symbol delay. Fig. 10 shows the simulation results on required OSNR for BER=10^{-3} versus symbol delay between X/Y polarizations set at the transmitter. The transmission line is the same as in Figure 7.9; distributed dispersion map with launch power of +1.3 dBm. As seen in Figure 7.9, the RZ formats are more sensitive to symbol delay misalignment compared with NRZ because they also benefit the most from symbol-interleaving. For RZ formats, we observe a degradation of ~ 0.5 dB when the symbol-interleaving is misaligned by ~ 15% of a symbol period.

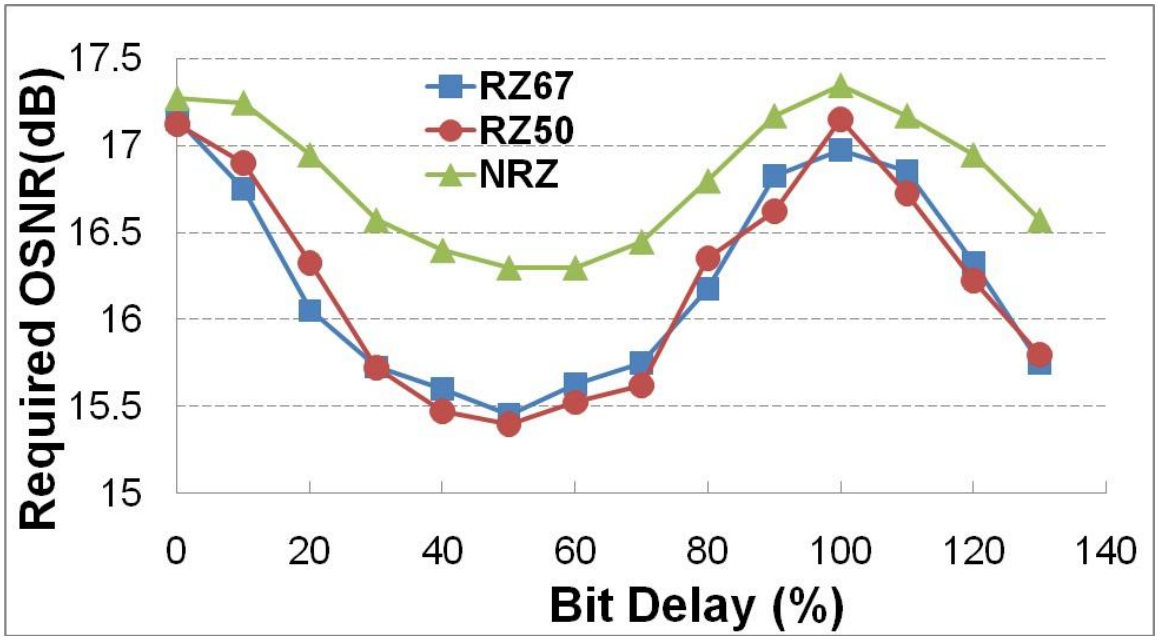

Figure 7.10 Impact of optical filtering in the linear regime.

7.5 Summary & Conclusions

The interaction of signal pulse shape with the optical line system dispersion map plays an important role in the nonlinear transmission performance of 100G DP-QPSK systems. Symbol-interleaving can be a very effective technique for fiber nonlinearity management

on distributed dispersion maps, where the pulse shape is well preserved during transmission. In this case, we have shown that 50% duty cycle RZ pulses are not required to obtain the maximum benefit from symbol-interleaving; the spectrally more efficient 67% duty cycle RZ pulses would be nearly as effective, and even NRZ pulses obtain a significant benefit from symbol-interleaving. The lumped dispersion map shows the overall best performance in suppressing fiber nonlinear effects, with only a weak dependence on pulse shape and/or symbol-interleaving.

The RZ pulse shape shows the greatest improvement in nonlinear tolerance with symbol-interleaving. However, symbol-interleaving only provides significant benefit in optical line systems designed to preserve the pulse shape during transmission, such as systems based on distributed dispersion compensating fiber (DCF). The duty cycle of the RZ pulse has a minor impact on nonlinear performance, and even systems based on the NRZ pulse shape can gain significant benefit from symbol-interleaving. The comparison of QPSK pulse shapes presents an interesting trade-off between spectral efficiency and nonlinear tolerance.

Chapter 8
Conclusions and Visions

A large amount of data exchanges induces internet traffic, consumes telecommunication network bandwidths, as well as accelerates the development of fiber-optic communications. Four years ago, 40-Gb/s optical transmission system was just targeted to be accomplished, and it became commercially possible in 2008. Dramatically in 2009, 100-Gb/s optical transmission system was developed because of digital coherent detection. In such a rapid revolution of leading system capacities toward 40 Gb/s or 100 Gb/s in single-channel, the nonlinear phase noise caused by optical fiber nonlinearities played an important role for system design, especially for phase-sensitive modulation formats such as DQPSK or QPSK. Thus, realizing the nonlinear tolerance of high spectral efficiency modulation formats, dispersion compensation maps, or different receiver schemes is quite helpful for system designers.

In the first few chapters, we reviewed the tolerances to linear and nonlinear impairments for different modulation formats, such as optical duobinary, DQPSK, and QPSK, in experiments and in simulations. Moreover, this thesis includes the studies for both conventional and our novel receiver structures in duobinary and DQPSK formats. This chapter would summarize these results combined with the references quoted in previous chapters into several ways of comparison: 1) spectral efficiency or pulse spectra, 2)

OSNR sensitivity, 3) chromatic dispersion, 4) Gordon-Mollenauer (GM) phase noise tolerance, and 5) complexity.

A novel lower-complexity DQPSK receiver based on frequency discriminator (FD-DD) was demonstrated experimentally, while also displaying a 4dB higher tolerance to nonlinear phase noise induced by Gordon-Mollenauer Effects and 2x fiber chromatic dispersion tolerance compared with the conventional receiver based on delay-interferometer (DI-BD). Similar to the advantages of our proposed receiver (FD-DD) in DQPSK system, a small benefit also appears in Polarization Division Multiplexing (Polmux) DQPSK system. Following the experimental results in the two different phase modulation systems, the possible beauty for cross phase modulation, a better tolerance to noise from crosstalk between channels, could be expected on the receiver based on frequency discriminator demodulator in the future.

The RZ pulse shape shows the greatest improvement in nonlinear tolerance with symbol-interleaving. However, symbol-interleaving only provides significant benefit in optical line systems designed to preserve the pulse shape during transmission, such as systems based on distributed dispersion compensating fiber (DCF). The duty cycle of the RZ pulse has a minor impact on nonlinear performance, and even systems based on the NRZ pulse shape can gain significant benefit from symbol-interleaving. The comparison of QPSK pulse shapes presents an interesting trade-off between spectral efficiency and nonlinear tolerance.

To sum up, recent advances of QPSK modulation with digital coherent receiver demonstrates outlines a well-developed future blue print of fiber-optic communications. The digital coherent detection allows demultiplexing polarization in the electrical domain, providing efficient equalization of linear impairments, such as dispersion and PMD, as well. For a long-haul transmission, multi-level modulation supports spectral efficient transmission. However, cross phase modulation induced by near channels carries on the nonlinear transmission effects like nonlinear polarization scattering or cross polarization modulation (XPOLM). Therefore, as the nonlinearities caused by the crosstalk between polarizations or neighboring channels can be efficiently reduced, a multi-level modulation combined with digital coherent receiver could relieve the internet traffic in the future.

References

[1] B. Mukherjee, "Optical WDM networks," in *Optical networks series*, [Enl. and rev. ed. New York: Springer, 2006, pp. xliii, 953 p. ill. 26 cm.

[2] J. M. Kahn and H. Keang-Po, "Spectral efficiency limits and modulation/detection techniques for DWDM systems," *Selected Topics in Quantum Electronics, IEEE Journal of*, vol. 10, pp. 259-272, 2004.

[3] *IEEE 802.3 Higher Speed Study Group*. Available: http://www.ieee802.org/3/hssg/index.html

[4] *IEEE P802.3ba 40Gb/s and 100Gb/s Ethernet Task Force Public Area*. Available: http://grouper.ieee.org/groups/802/3/ba/public/

[5] Cisco Visual Networking Index: Forecast and Methodology, 2009-2014. Available: http://www.cisco.com/en/US/solutions/collateral/ns341/ns525/ns537/ns705/ns827/white_paper_c11-481360.pdf

[6] Hyperconnectivity and the Approaching Zettabyte Era. Available: http://www.cisco.com/en/US/solutions/collateral/ns341/ns525/ns537/ns705/ns827/VNI_Hyperconnectivity_WP.pdf

[7] "Youtube."

[8] *Facebook*. Available: http://www.facebook.com/

[9] K. M. Sivalingam, S. Subramaniam, and I. ebrary, *Optical WDM networks principles and practice*. New York: Kluwer Academic, 2002.

[10] G. P. Agrawal, *Fiber-optic communication systems*, 4th ed. Hoboken, N.J.: Wiley, 2010.

[11] M. W. Chbat and D. Penninckx, "High-spectral-efficiency transmission systems," in *Optical Fiber Communication Conference, 2000*, 2000, pp. 134-136 vol.1.

[12] A. H. Gnauck, G. Charlet, P. Tran, P. J. Winzer, C. R. Doerr, J. C. Centanni, E. C. Burrows, T. Kawanishi, T. Sakamoto, and K. Higuma, "25.6-Tb/s WDM Transmission of Polarization-Multiplexed RZ-DQPSK Signals," *Lightwave Technology, Journal of*, vol. 26, pp. 79-84, 2008.

[13] P. J. Winzer, G. Raybon, H. Song, A. Adamiecki, S. Corteselli, A. H. Gnauck, D. A. Fishman, C. R. Doerr, S. Chandrasekhar, L. L. Buhl, T. J. Xia, G. Wellbrock, W. Lee, B. Basch, T. Kawanishi, K. Higuma, and Y. Painchaud, "100-Gb/s DQPSK Transmission: From Laboratory Experiments to Field Trials," *J. Lightwave Technol.*, vol. 26, pp. 3388-3402, 2008.

[14] S. Chandrasekhar and X. Liu, "Impact of Channel Plan and Dispersion Map on Hybrid DWDM Transmission of 42.7-Gb/s DQPSK and 10.7-Gb/s OOK on 50-GHz Grid," *Photonics Technology Letters, IEEE*, vol. 19, pp. 1801-1803, 2007.

[15] A. D. Ellis, Z. Jian, and D. Cotter, "Approaching the Non-Linear Shannon Limit," *Lightwave Technology, Journal of*, vol. 28, pp. 423-433, 2010.

[16] K. C. K. a. G. A. Hockham, "Dielectric-Fiber Surface Waveguides for Optical Frequencies," *Proc. Inst. Elect. Eng.*, vol. 113, p. 7, Jul. 1966.

[17] E. Desurvire, *Erbium-doped fiber amplifiers : principles and applications*. New York: Wiley, 1994.

[18] A. Bjarklev, *Optical fiber amplifiers : design and system applications*. Boston: Artech House, 1993.
[19] D. N. Payne and L. Reekie, "Rare-earth-doped fibre lasers and amplifiers," in *Optical Communication, 1988. (ECOC 88). Fourteenth European Conference on (Conf. Publ. No.292)*, 1988, pp. 49-53 vol.1.
[20] C. Lin, H. Kogelnik, and L. G. Cohen, "Optical-pulse equalization of low-dispersion transmission in single-mode fibers in the 1.3?1.7-µm spectral region," *Opt. Lett.*, vol. 5, pp. 476-478, 1980.
[21] (2007). *Springer handbook of lasers and optics*.
[22] G. P. Agrawal, *Nonlinear fiber optics*, 4th ed. Burlington, MA ; London: Academic Press, 2007.
[23] A. Demir, "Nonlinear Phase Noise in Optical-Fiber-Communication Systems," *Lightwave Technology, Journal of*, vol. 25, pp. 2002-2032, 2007.
[24] N. B. Delone and V. P. Kra*inov, *Fundamentals of nonlinear optics of atomic gases*. New York: Wiley, 1988.
[25] Y. K. Lize, X. Wu, M. Nazarathy, Y. Atzmon, L. Christen, S. Nuccio, M. Faucher, N. Godbout, and A. E. Willner, "Chromatic dispersion tolerance in optimized NRZ-, RZ- and CSRZ-DPSK demodulation," *Opt. Express*, vol. 16, pp. 4228-4236, 2008.
[26] J. M. Dziedzic, R. H. Stolen, and A. Ashkin, "Optical Kerr effect in long fibers," *Appl. Opt.*, vol. 20, pp. 1403-1406, 1981.
[27] R. H. Stolen and C. Lin, "Self-phase-modulation in silica optical fibers," *Physical Review A*, vol. 17, p. 1448, 1978.
[28] J. P. Gordon and L. F. Mollenauer, "Phase noise in photonic communications systems using linear amplifiers," *Opt. Lett.*, vol. 15, pp. 1351-1353, 1990.
[29] E. Desurvire, "Capacity Demand and Technology Challenges for Lightwave Systems in the Next Two Decades," *Lightwave Technology, Journal of*, vol. 24, pp. 4697-4710, 2006.
[30] D. van den Borne, S. L. Jansen, E. Gottwald, P. M. Krummrich, G. D. Khoe, and H. de Waardt, "1.6-b/s/Hz Spectrally Efficient Transmission Over 1700 km of SSMF Using 40 × 85.6-Gb/s POLMUX-RZ-DQPSK," *Lightwave Technology, Journal of*, vol. 25, pp. 222-232, 2007.
[31] A. H. Gnauck and P. J. Winzer, "Optical phase-shift-keyed transmission," *Lightwave Technology, Journal of*, vol. 23, pp. 115-130, 2005.
[32] A. Lender, "The duobinary technique for high-speed data transmissio," *IEEE Trans. Commun. Electron.*, vol. 82, May, 1963.
[33] A. Lender, "Correlative Digital Communication Techniques," *Communication Technology, IEEE Transactions on*, vol. 12, pp. 128-135, 1964.
[34] G. Bosco, A. Carena, V. Curri, R. Gaudino, and P. Poggiolini, "Modulation formats suitable for ultrahigh spectral efficient WDM systems," *Selected Topics in Quantum Electronics, IEEE Journal of*, vol. 10, pp. 321-328, 2004.
[35] S. Bigo, "Multiterabit/s DWDM terrestrial transmission with bandwidth-limiting optical filtering," *Selected Topics in Quantum Electronics, IEEE Journal of*, vol. 10, pp. 329-340, 2004.

[36] N. B. Pavlovic and A. V. T. Cartaxo, "Influence of Tight Optical Filtering on Long-Haul Transmission Performance of Several Advanced Signaling Formats," *Lightwave Technology, Journal of*, vol. 26, pp. 1339-1348, 2008.

[37] A. Tan and E. Pincemin, "Performance Comparison of Duobinary Formats for 40-Gb/s and Mixed 10/40-Gb/s Long-Haul WDM Transmission on SSMF and LEAF Fibers," *Lightwave Technology, Journal of*, vol. 27, pp. 396-408, 2009.

[38] K. Hoon and C. X. Yu, "Optical duobinary transmission system featuring improved receiver sensitivity and reduced optical bandwidth," *Photonics Technology Letters, IEEE*, vol. 14, pp. 1205-1207, 2002.

[39] P. Brindel, L. Pierre, G. Ducournau, O. Latry, M. Ketata, and O. Leclerc, "Optical generation of 43 Gbit/s phase-shaped binary transmission format from DPSK signal using 50 GHz periodic optical filter," in *Optical Communication, 2005. ECOC 2005. 31st European Conference on*, 2005, pp. 847-848 vol.4.

[40] P. J. Winzer and R. J. Essiambre, "Advanced Modulation Formats for High-Capacity Optical Transport Networks," *Lightwave Technology, Journal of*, vol. 24, pp. 4711-4728, 2006.

[41] A. H. Gnauck, P. J. Winzer, C. Dorrer, and S. Chandrasekhar, "Linear and nonlinear performance of 42.7-Gb/s single-polarization RZ-DQPSK format," *Photonics Technology Letters, IEEE*, vol. 18, pp. 883-885, 2006.

[42] M. Daikoku, I. Morita, H. Taga, H. Tanaka, T. Kawanishi, T. Sakamoto, T. Miyazaki, and T. Fujita, "100-Gb/s DQPSK Transmission Experiment Without OTDM for 100G Ethernet Transport," *J. Lightwave Technol.*, vol. 25, pp. 139-145, 2007.

[43] H. G. Weber, S. Ferber, M. Kroh, C. Schmidt-Langhorst, R. Ludwig, V. Marembert, C. Boerner, F. Futami, S. Watanabe, and C. Schubert, "Single channel 1.28 Tbit/s and 2.56 Tbit/s DQPSK transmission," *Electronics Letters*, vol. 42, pp. 178-179, 2006.

[44] I. Lyubomirsky and B. Pitchumani, "Impact of optical filtering on duobinary transmission," *Photonics Technology Letters, IEEE*, vol. 16, pp. 1969-1971, 2004.

[45] C. Malouin, J. Bennike, and T. Schmidt, "DPSK Receiver Design - Optical Filtering Considerations," in *Optical Fiber Communication and the National Fiber Optic Engineers Conference, 2007. OFC/NFOEC 2007. Conference on*, 2007, pp. 1-3.

[46] D. Penninckx, M. Chbat, L. Pierre, and J. P. Thiery, "The phase-shaped binary transmission (PSBT): a new technique to transmit far beyond the chromatic dispersion limit," *Photonics Technology Letters, IEEE*, vol. 9, pp. 259-261, 1997.

[47] M. Sieben, J. Conradi, and D. E. Dodds, "Optical single sideband transmission at 10 Gb/s using only electrical dispersion compensation," *Lightwave Technology, Journal of*, vol. 17, pp. 1742-1749, 1999.

[48] P. J. Winzer and R. J. Essiambre, "Advanced Optical Modulation Formats," *Proceedings of the IEEE*, vol. 94, pp. 952-985, 2006.

[49] D. M. Gill, A. H. Gnauck, L. Xiang, W. Xing, D. S. Levy, S. Chandrasekhar, and C. R. Doerr, "42.7-Gb/s cost-effective duobinary optical transmitter using a

commercial 10-Gb/s Mach-Zehnder modulator with optical filtering," *Photonics Technology Letters, IEEE,* vol. 17, pp. 917-919, 2005.

[50] P. J. Winzer, S. Chandrasekhar, C. R. Doerr, D. T. Neilson, A. Adamiecki, and R. A. Griffin, "42.7-Gb/s Modulation with a Compact InP Mach-Zehnder Transmitter," in *Optical Communications, 2006. ECOC 2006. European Conference on*, 2006, pp. 1-2.

[51] Y. K. Lize, W. Xiaoxia, L. Christen, M. Faucher, and A. E. Willner, "Free Spectral Range and Optical Filtering Optimization in NRZ-, RZ- and CSRZ-DPSK demodulation," in *Lasers and Electro-Optics Society, 2007. LEOS 2007. The 20th Annual Meeting of the IEEE*, 2007, pp. 139-140.

[52] Y. K. Lizé, L. Christen, X. Wu, J.-Y. Yang, S. Nuccio, T. Wu, A. E. Willner, and R. Kashyap, "Free spectral range optimization of return-to-zero differential phase shift keyed demodulation in the presence of chromatic dispersion," *Opt. Express,* vol. 15, pp. 6817-6822, 2007.

[53] A. Tan and E. Pincemin, "Performance Comparison of Duobinary Formats for 40-Gb/s and Mixed 10/40-Gb/s Long-Haul WDM Transmission on SSMF and LEAF Fibers," *J. Lightwave Technol.,* vol. 27, pp. 396-408, 2009.

[54] J. D. Downie, J. Hurley, and M. Sauer, "Behavior of MLSE-EDC With Self-Phase Modulation Limitations and Various Dispersion Levels in 10.7-Gb/s NRZ and Duobinary Signals," *Photonics Technology Letters, IEEE,* vol. 19, pp. 1017-1019, 2007.

[55] T. Ono, Y. Yano, K. Fukuchi, T. Ito, H. Yamazaki, M. Yamaguchi, and K. Emura, "Characteristics of optical duobinary signals in terabit/s capacity, high-spectral efficiency WDM systems," *Lightwave Technology, Journal of,* vol. 16, pp. 788-797, 1998.

[56] P. Erwan, G. Christophe, D. Laurent, T. Antoine, and B. Aude, "Experimental Performance Comparison of Duobinary Formats for 40 Gb/s Long-Haul Transmission," 2008, p. JThA55.

[57] G. Bosco and P. Poggiolini, "On the joint effect of receiver impairments on direct-detection DQPSK systems," *Lightwave Technology, Journal of,* vol. 24, pp. 1323-1333, 2006.

[58] K. Hoon and P. J. Winzer, "Robustness to laser frequency offset in direct-detection DPSK and DQPSK systems," *Lightwave Technology, Journal of,* vol. 21, pp. 1887-1891, 2003.

[59] H. Keang-Po, "The effect of interferometer phase error on direct-detection DPSK and DQPSK signals," *Photonics Technology Letters, IEEE,* vol. 16, pp. 308-310, 2004.

[60] I. Lyubomirsky, C. Cheng-Chung, and W. Yi-Hsiang, "Optical DQPSK Receiver With Enhanced Dispersion Tolerance," *Photonics Technology Letters, IEEE,* vol. 20, pp. 511-513, 2008.

[61] C. R. S. Fludger, T. Duthel, D. van den Borne, C. Schulien, E. D. Schmidt, T. Wuth, J. Geyer, E. De Man, G.-D. Khoe, and H. de Waardt, "Coherent Equalization and POLMUX-RZ-DQPSK for Robust 100-GE Transmission," *Lightwave Technology, Journal of,* vol. 26, pp. 64-72, 2008.

[62] J. Renaudier, O. Bertran-Pardo, G. Charlet, M. Salsi, M. Bertolini, P. Tran, H. Mardoyan, and S. Bigo, "Investigation on WDM Nonlinear Impairments Arising From the Insertion of 100-Gb/s Coherent PDM-QPSK Over Legacy Optical Networks," *Photonics Technology Letters, IEEE,* vol. 21, pp. 1816-1818, 2009.

[63] V. Curri, P. Poggiolini, A. Carena, and F. Forghieri, "Dispersion Compensation and Mitigation of Nonlinear Effects in 111-Gb/s WDM Coherent PM-QPSK Systems," *Photonics Technology Letters, IEEE,* vol. 20, pp. 1473-1475, 2008.

[64] X. Chongjin, "Interchannel Nonlinearities in Coherent Polarization-Division-Multiplexed Quadrature-Phase-Shift- Keying Systems," *Photonics Technology Letters, IEEE,* vol. 21, pp. 274-276, 2009.

[65] C. Xie, "WDM coherent PDM-QPSK systems with and without inline optical dispersion compensation," *Opt. Express,* vol. 17, pp. 4815-4823, 2009.

[66] P. J. Winzer and A. Kalmar, "Sensitivity Enhancement of Optical Receivers by Impulsive Coding," *J. Lightwave Technol.,* vol. 17, p. 171, 1999.

[67] R. Noe, "PLL-free synchronous QPSK polarization multiplex/diversity receiver concept with digital I&Q baseband processing," *Photonics Technology Letters, IEEE,* vol. 17, pp. 887-889, 2005.

[68] S. J. Savory, G. Gavioli, R. I. Killey, and P. Bayvel, "Electronic compensation of chromatic dispersion using a digital coherent receiver," *Opt. Express,* vol. 15, pp. 2120-2126, 2007.

Publications

1. Y.-H. Wang and I. Lyubomirsky, ***"Balanced Detection Schemes for Optical Duobinary Communication Systems,"*** IEEE Journal of Lightwave Technology, accepted March, 2011.
2. Y.-H. Wang and I. Lyubomirsky, ***"Impact of DP-QPSK Pulse Shape in Nonlinear 100 G Transmission,"*** IEEE Journal of Lightwave Technology, vol. 28, pp. 2750-2756, 2010.
3. C.-C. Cheng, Y. K. Lize, Y.-H. Wang, and I. Lyubomirsky, ***"Experimental Demonstration of Optical DQPSK Receiver Based on Frequency Discriminator Demodulator,"*** IEEE JLT, vol. 27, pp. 4228-4232, 2009.
4. I. Lyubomirsky, Y.-H. Wang, and C.-C. Cheng, ***"Low complexity optical DQPSK receiver with enhanced tolerance to transmission impairments,"*** in Lasers and Electro-Optics, CLEO/QELS 2009, pp. 1-2.
5. I. Lyubomirsky, C.-C. Cheng, and Y.-H. Wang, ***"Optical DQPSK Receiver with Enhanced Dispersion Tolerance,"*** IEEE Photonics Technology Letters, vol. 20, pp. 511-513, 2008.